Supplemental Material for:

Design of symmetrical and nonsymmetrical *N,N*-dimethylaminopyridine derivatives as highly potent choline kinase alpha inhibitors

Sebastian Trousil, Laurence Carroll,* Andrew Kalusa, Maciej Kaliszczak and Eric O. Aboagye

email: l.carroll@imperial.ac.uk

Table of Contents

1. Supplementary Figures and Tables

A **B**

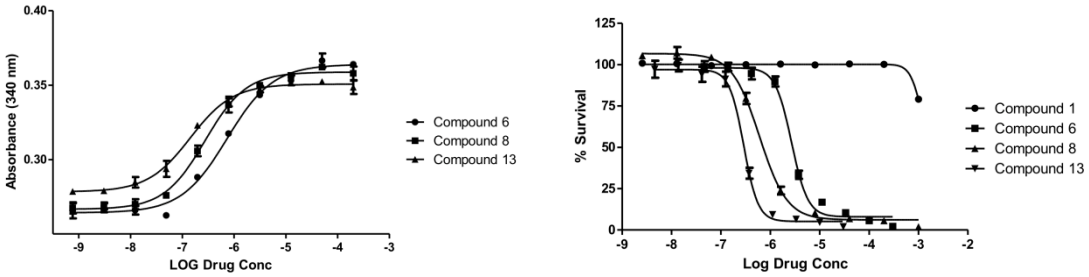

Supplementary Figure 1. Exemplary curves demonstrating inhibition of Δ49N CHKA2 and growth of human HCT116 or A549 cancer cell lines. (A) IC_{50} was determined using a pyruvate kinase/lactate dehydrogenase-coupled assay that measures NADH depletion at 340 nm. High NADH levels reflect complete enzymatic inhibition. (B) GI_{50} was determined by sulforhodamine-B assay. For both assays, half-maximal inhibitory concentrations were determined by fitting of a sigmoidal curve with variable slope in GraphPad Prism version 5.01.

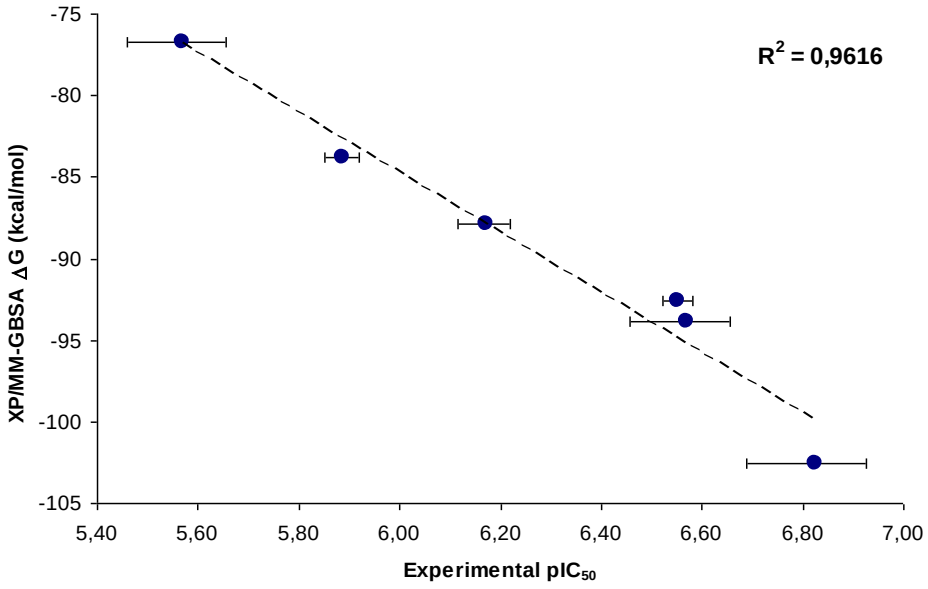

Supplementary Figure 2. Correlation for compound **3**, **5**, **6**, **7**, **8** and **13** between experimental pIC_{50} against Δ49N CHKA2 and estimated free energies of binding (kcal/mol) obtained by Glide XP docking and MM-GBSA scoring.

Supplementary Table 1. Different scoring functions applied to SP and XP docked poses.

Compound	Linker	IC_{50} (μM)	pIC_{50}	SP Docking Score	SP/MM-GBSA (kcal/mol)	XP Docking Score	XP/MM-GBSA (kcal/mol)	Comment
3[a]	C8	2.7	5.57	-6.924	-74.00	-5.210	-76.68	Only choline competitive
5[a]	C9	1.3	5.89	-6.806	-80.50	-8.825	-83.77	
6[a]	C10	0.68	6.17	-8.017	-87.72	-7.927	-87.89	
7[a]	C11	0.29	6.55	-6.739	-88.87[f]	-5.174[f]	-92.61[f]	
8[a]	C12	0.27	6.57	-7.688	-83.18	-7.860	-93.84	
13[a]	C14	0.15	6.82	-6.563	-101.1	-6.955	-102.5	
9[c, d]	C12	5.0	5.30	-6.512[a]	-87.93[a]	-8.430[b]	-75.22[b]	Mixed binding mode
9[c, e]				-5.095[b]	-84.10[b]	-5.802[a]	-70.28[a]	
10[b]	C12	0.34	6.47	-9.643	-91.18	-5.484	-69.42	
12[b]	C12	0.80	6.10	-7.083	-84.71	-7.170	-68.95	

[a]Docks simultaneously in the choline site and the pocket rim in the highest ranked pose [b]Docks simultaneously in the choline site and in the ATP site in the highest ranked pose. [c]The calculated pK_a of the benzimidazole moiety is 5.62. [d]Neutral. [e]Protonated. [f]XP docking resulted in an unrealistic pose, instead the XP refined SP docked pose was used.

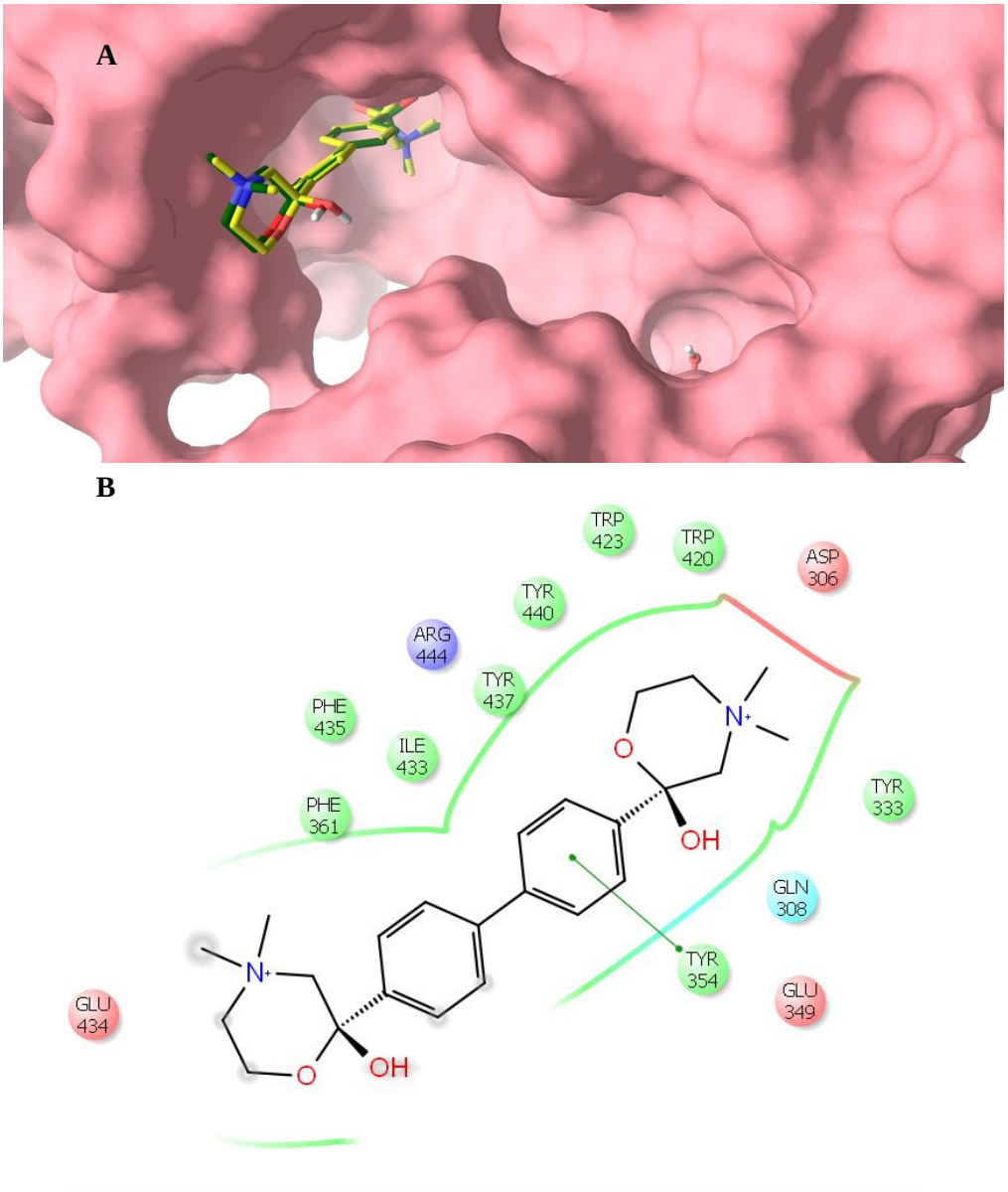

Supplementary Figure 3: (A) the applied docking algorithm could successfully dock hemicholinium-3. The docked molecule (green) overlays with the co-crystallised ligand (yellow). (B) Close-contact interactions of hemicholinium-3 with CHKA2.

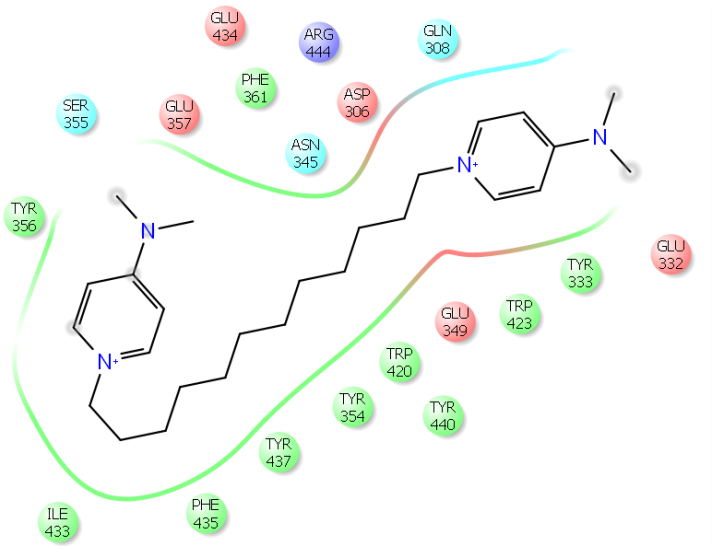

Supplementary Figure 4: Interactions of **8** in its most stable pose with the choline pocket and rim of CHKA2.

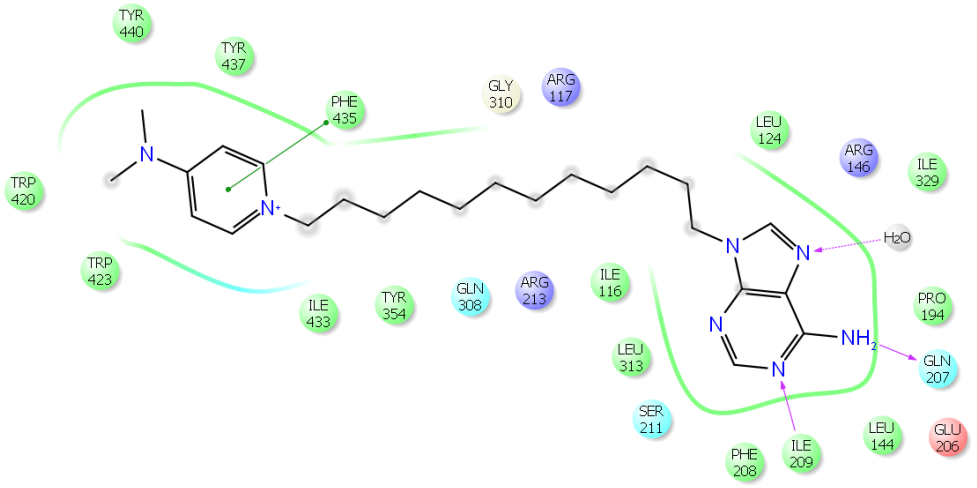

Supplementary Figure 5: Interactions of **12** in its most stable pose with the ATP cassette and the choline pocket.

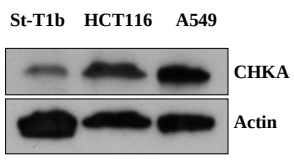

Supplementary Figure 6: HCT116 and A549 cells express CHKA at high levels compared to the endometrial stromal cell line St-T1b, as determined by western blotting.

2. General chemical procedures, materials and Instrumentation

All reactions were performed under anhydrous conditions and an atmosphere of nitrogen in flame-dried glassware unless otherwise stated. Yields refer to chromatographically and spectroscopically (^{1}H-NMR) homogenous materials.

Solvents and reagents: All solvents were purified and dried according to standard methods prior to use. All chemicals were handled in accordance with COSHH regulations. All reagents were used as commercially supplied.

Flash chromatography (FC) was always performed on silica gel (Merck Kieselgel 60 F_{254} 320-400 mesh) according to the method of W. C. Still, unless otherwise stated. Thin Layer Chromatography (TLC) was performed on Merck aluminium-backed plated pre-coated with silica (0.2 mm, 60 F_{254}) which were visualised either by quenching of ultraviolet fluorescence (λ = 254 and 366 nm) or by charring with 10% $KMnO_4$ in 1M H_2SO_4. ^{1}H NMR spectra: These were recorded at 400 MHz on a Bruker AV-400 or on a Bruker AV-500 instrument. Chemical shifts (δ_H) are quoted in parts per million (ppm), referenced to the appropriate residual solvent peak. Coupling constants (*J*) are reported to the nearest 0.5 Hz. ^{13}C NMR spectra: These were recorded at 100 MHz on a Bruker AV-400 or on a Bruker AV-500 instrument. Chemical shifts (δ_C) are quoted in ppm, referenced to the appropriate residual solvent peak. Mass spectra: Low resolution mass spectra (*m/z*) were recorded on either a VG platform II or VG AutoSpec spectrometers, with only molecular ions (M^+, MH^+, MNa^+, MK^+, MNH_4^+) and major peaks being reported with intensities quoted as percentages of the base peak. Analytical reverse-phase HPLC was carried out on a Beckmann Pump 127 instrument using a Phenomenex Gemini C18 column (150 mm x 4.6 mm) with a gradient of acetonitrile and water. Laura 3 software was used for processing all HPLC chromatograms.

2. Synthetic Procedures

General Procedure for the Synthesis of Mono-dimethylaminopyridine Linkers

1,12-Dibromododecane (2 mmol, 656 mg) was dissolved in 2-butanone (40 ml) and to that, 4-dimethylaminopyridine (1 mmol, 122 mg) was added. The reaction mixture was stirred for 3 hours at 110^{o}C, at which time a white precipitate formed. The precipitate was filtered and washed with 2-butanone (3 x 30 ml) and then diethyl ether (2 x 30 ml) before being dried *in vacuo* to give the desired product as a white solid (257 mg, 57 % yield).

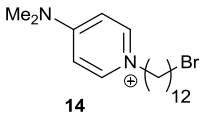

14

Yield = 57 %; δ_H (400 MHz, DMSO-D_6) 1.13-1.40 (16H, m), 1.69-1.82 (4H, m), 3.18 (6H, s), 3.57 (2H, t, *J* = 6.4 Hz), 4.14 (2H, t, *J* = 6.8 Hz), 7.03 (2H, d, *J* = 7.3 Hz), 8.28 (2H, d, *J* = 7.3 Hz); δ_C (100 MHz, DMSO-D_6) 25.9, 28.0, 28.6, 28.9, 29.0, 29.4, 29.9, 30.8, 32.7, 35.7, 36.4, 57.1, 108.2, 142.5, 156.3; *m/z* (EI^+) ($[M\text{-}Br^-]^+$) calcd. for 369.1900, found: 369.1890.

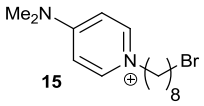

15

Yield = 47 %; δ_H (400 MHz, DMSO-D_6) 1.15-1.40 (8H, m), 1.70-1.83 (4H, m), 3.19 (6H, s), 3.53 (2H, dt, *J* = 6.4, 1.9 Hz), 4.17 (2H, t, *J* = 6.9 Hz), 7.03 (2H, d, *J* = 7.8 Hz), 8.35 (2H, d, *J* = 7.8 Hz); δ_C (100 MHz, DMSO-D_6) 25.8, 25.9, 27.9, 28.4, 28.7, 28.8, 30.8, 32.6, 35.7, 57.0, 108.2, 142.5, 156.3; *m/z* (EI^+) ($[M\text{-}Br^-]^+$) calcd. for 313.1724, found: 313.1724.

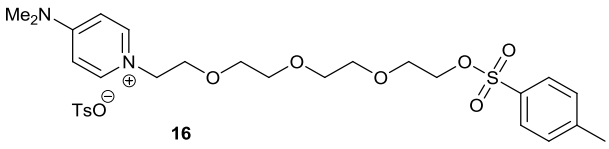

16

Yield = 64 %; δ_H (400 MHz, DMSO-D_6) 2.28 (3H, s), 2.42 (3H, s), 3.17 (6H, s), 3.39-3.45 (6H, m), 3.46-3.53 (2H, m), 3.54-3.58 (2H, m), 3.74 (2H, dt, *J* = 9.8, 4.4 Hz), 4.10 (2H, t, *J* = 4.4 Hz), 4.29-4.34 (2H, m), 6.99-7.04 (2H, m), 7.12 (2H, d, *J* = 7.8 Hz), 7.49 (4H, d, *J* = 7.8 Hz), 7.70-7.81 (2H, m), 8.21-8.26 (2H, m); δ_C (100 MHz, DMSO-D_6) 21.3, 21.6, 55.8, 68.4, 69.5, 70.0, 70.1, 70.2, 70.5, 107.8, 125.9, 128.1, 128.5, 130.6, 138.0, 142.9, 146.4, 156.4; *m/z* (EI^+) ($[M\text{-}TsO^-]^+$) calcd. for 453.2054, found: 453.2050.

General Procedure for the Synthesis of *Bis*-dimethylaminopyridine Compounds

1,12-Dibromododecane (0.5 mmol, 164 mg) was dissolved in 2-butanone (10 ml) and to that, 4-dimethylaminopyridine (1 mmol, 122 mg) was added. The reaction mixture was stirred for 3 hours at 110^{o}C, at which time a white precipitate formed. The precipitate was filtered and washed with 2-butanone (3 x 10 ml) and then diethyl ether (2 x 15 ml) before being dried *in vacuo* to give the desired product as a white solid (270 mg, 94 % yield).

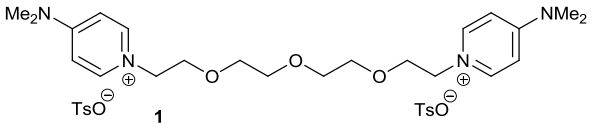

1

Yield = 88 %; δ_H (400 MHz, DMSO-D_6) 2.36 (6H, s), 3.19 (12H, s), 3.55 (8H, dm, *J* = 19.1 Hz), 3.81 (4H, t, *J* = 4.9 Hz), 4.31 (4H, t, *J* = 4.9 Hz), 4.87 (6H, s), 6.91 (4H, d, *J* = 7.8 Hz), 7.23 (4H, d, *J* = 7.8 Hz), 7.72 (4H, d, *J* = 7.8 Hz), 8.12 (4H, d, *J* = 7.8 Hz); δ_C (100 MHz, DMSO-D_6) 29.7, 30.8, 48.9, 61.0, 61.8, 61.9, 99.0, 117.4, 120.3, 132.0, 134.1, 139.6, 148.3; *m/z* (EI^+) ($[M\text{-}TsO^-]^{2+}$) 202.1.

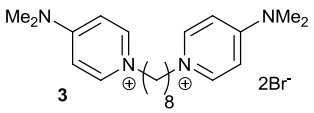

3

Yield = 86 %; δ_H (400 MHz, DMSO-D_6) 1.15-1.31 (8H, m), 1.69-1.81 (4H, m), 3.19 (12, s), 4.18 (4H, t, *J* = 7.3 Hz, 7.05 (4H, d, *J* = 7.8 Hz), 8.35 (4H, d, *J* = 7.8 Hz); δ_C (100 MHz, DMSO-D_6) 25.8, 28.8, 30.8, 35.7, 57.0, 108.2, 142.5, 156.3; *m/z* (EI^+) ($[M\text{-}Br^-]^{2+}$ 178.1.

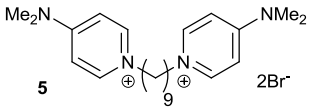

5

Yield = 88 %; δ_H (400 MHz, DMSO-D_6) 1.05-1.52 (10H, m), 1.63-1.95 (4H, m), 3.19 (12H, s), 4.16 (4H, t, *J* = 7.2 Hz), 6.99-7.11 (4H, m), 8.29-8.39 (4H, m); δ_C (100 MHz, DMSO-D_6) 25.9, 28.8, 29.2, 30.8, 57.1, 108.10, 108.14, 142.43, 142.47, 156.3; *m/z* (EI^+) ($[M\text{-}Br^-]^{2+}$ 185.2.

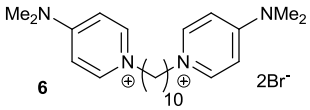

6

Yield = 63%; δ_H (400 MHz, DMSO-D_6) 1.23 (12H, as), 1.61-2.00 (4H, m), 3.19 (12H, s), 4.17 (4H, t, *J* = 7.2 Hz), 7.05 (4H, d, *J* = 7.7 Hz), 8.35 (4H, d, *J* = 7.7 Hz); δ_C (100 MHz, DMSO-D_6) 25.9, 28.9, 29.3, 30.8, 57.1, 108.1, 142.5, 156.3; *m/z* (EI^+) ($[M\text{-}Br^-]^{2+}$ 192.2.

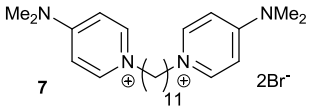

7

Yield = 84%; δ_H (400 MHz, DMSO-D_6) 1.22 (14H, s), 1.64-1.93 (4H, m), 3.19 (12H, s), 4.18 (4H, t, *J* = 7.2 Hz), 6.99-7.11 (4H, m), 8.31-8.42 (4H, m); δ_C (100 MHz, DMSO-D_6) 25.9, 28.9, 29.3, 30.8, 57.0, 108.1, 142.5, 156.3; *m/z* (EI^+) ($[M\text{-}Br^-]^{2+}$ 220.0.

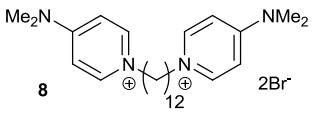

8

Yield = 94 %; δ_H (400 MHz, DMSO-D_6) 1.12-1.31 (16H, m,), 1.67-1.82 (4H, m), 3.19 (12H, s), 4.17 (4H, t, *J* = 7.3 Hz), 7.05 (4H, d, *J* = 7.8 Hz), 8.34 (4H, d, *J* = 7.8 Hz); δ_C (100 MHz, DMSO-D_6) 25.9, 28.9, 29.3, 29.37, 29.41, 30.8, 50.1, 108.2, 142.5, 156.3; *m/z* (EI^+) ($[M\text{-}Br^-]^{2+}$) 206.2.

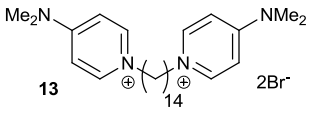

13

Yield = 81%; δ_H (400 MHz, DMSO-D_6) 1.12-1.50 (20H, m), 1.75 (4H, dq, *J* = 14.4 Hz), 3.18 (12H, t, *J* = 7.2 Hz), 4.16 (4H, t, *J* = 7.2 Hz), 7.04 (4H, d, *J* = 7.8 Hz), 8.33 (4H, dd, *J* = 6.3, 4.6 Hz); *m/z* (EI^+) ($[M\text{-}Br^-]^{2+}$) 220.2.

General Procedure for the Synthesis of Asymmetrical ATP-Mimicking Compounds

To a stirred solution of compound **15** (392 mg, 1 mmol) in DMF (10 ml) was added K_2CO_3 (166 mg, 1.2 mmol) and then benzimidazole (118 mg, 1 mmol). The reaction mixture was heated to 130^{o}C for 16 hours, at which point it was concentrated *in vacuo*. The residue was purified by flash chromatography (95:5 to 80:20 DCM:MeOH) to afford the desired compound (279 mg, 65 % yield) as a yellow oil.

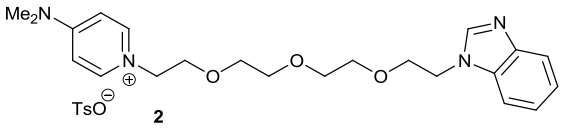

2

Yield = 46 %; δ_H (400 MHz, MeOD-D_4) 2.26 (3H, s), 2.41 (3H, s), 3.17 (6H, s), 3.39-3.45 (6H, m), 3.45-3.56 (2H, m), 3.54-3.58 (2H, m), 3.74 (2H, dt, *J* = 9.8, 4.4 Hz), 4.10 (2H, t, *J* = 4.4 Hz), 4.29-4.34 (2H, m), 6.99-7.04 (4H, m), 7.24-7.35 (4H, m), 7.60 (1H, d, *J* = 7.7 Hz), 7.65 (1H, d, *J* = 7.7 Hz), 8.13-8.27 (3H, m); δ_C (100 MHz, DMSO-D_6) 21.0, 21.8, 55.5, 68.3, 69.5, 70.0, 70.1, 70.3, 70.6, 107.6, 126.0, 128.0, 128.6, 128.7, 130.6, 138.1, 142.7, 146.4, 156.4; *m/z* (EI^+) ([M-TsO^-]$^+$) calcd. for 399.2391, found: 399.2389.

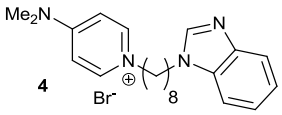

4

Yield = 65 %; δ_H (400 MHz, MeOD-D_4) 1.24-1.40 (8H, m), 1.78-1.94 (4H, m), 3.26 (6H, s), 4.16 (2H, t, *J* = 7.3 Hz), 4.32 (2H, t, *J* = 6.9 Hz), 6.99 (2H, d, *J* = 7.8 Hz), 7.27-7.37 (2H, m), 7.59 (1H, d, *J* = 7.8 Hz), 7.68 (1H, d, *J* = 7.8 Hz), 8.16-8.23 (3H, m); δ_C (100 MHz, MeOD-D_4) 25.5, 25.6, 28.5, 29.4, 30.4, 39.0, 44.6, 57.5, 107.6, 110.2, 118.7, 122.1, 122.8, 141.7, 143.4, 156.5; *m/z* (EI^+) ([M-Br^-]$^+$) calcd. for 351.2543, found: 351.2540.

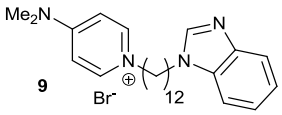

9

Yield = 72 %; δ_H (400 MHz, DMSO-D_6) 1.15-1.27 (16H, m), 1.68-1.83 (4H, m), 3.18 (6H, s), 4.13 (2H, t, *J* = 7.3 Hz), 4.23 (2H, t, *J* = 7.3 Hz), 7.02 (2H, d, *J* = 7.8 Hz), 7.17-7.26 (2H, m), 7.61 (2H, ddd, *J* = 21.0, 7.3, 1.0 Hz), 8.21 (1H, s), 8.29 (2H, d, *J* = 7.8 Hz); δ_C (100 MHz, MeOD-D_4) 25.8, 26.2, 28.6, 28.7, 29.05, 29.06, 29.3, 29.5, 30.5, 39.0, 43.6, 57.5, 107.6, 141.7, 147.15, 147.20, 151.8, 152.0, 156.5; *m/z* (EI^+) ([M-Br^-]$^+$) calcd. for 393.3013, found: 393.3013.

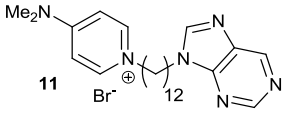

11

Yield = 54 % (3:1, inseparable mixture of N-3 and N-9 regioisomers); δ_H (400 MHz, MeOD-D_4) 1.21-1.37 (16H, m), 1.81-2.01 (4H, m), 3.27 (6H, s), 4.20 (2H, t, *J* = 7.3 Hz), 4.40 (1.5H, t, *J* = 7.3 Hz, N-3), 4.47 (0.5H, t, *J* = 7.3 Hz, N-9), 7.02 (2H, d, *J* = 7.8 Hz), 8.19 (2H, d, *J* = 7.8 Hz), 8.60 (0.75H, s, N-3), 8.71 (0.25H, s, N-9), 8.95 (0.75H, s, N-3), 9.02 (0.25H, s, N-9), 9.10 (0.75H, s, N-3), 9.25 (0.25H, s, N-9); δ_C (100 MHz, MeOD-D_4) 25.8, 26.2, 28.6, 29.1, 29.2, 29.3, 30.6, 38.9, 43.6, 57.6, 107.6, 141.7, 147.2, 151.8, 156.5; *m/z* (EI^+) ([M-Br^-]$^+$) calcd. for 395.2918, found: 395.2920.

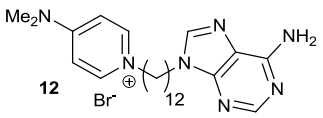

Yield = 61 %; δ_H (400 MHz, MeOD-D_4) 1.21-140 (16H, m), 1.82-1.93 (4H, m), 3.26 (6H, s), 4.18 (2H, t, *J* = 7.3 Hz), 4.25 (2H, t, *J* = 7.3 Hz), 7.00 (2H, d, *J* = 7.8 Hz), 8.14-8.21 (3H, m), 8.22 (1H, s); δ_C (100 MHz, MeOD-D_4) 25.8, 26.1, 28.6, 28.7, 29.0, 29.1, 29.6, 30.5, 38.9, 43.6, 57.6, 107.6, 141.4, 141.7, 152.2, 151.3, 156.5; *m/z* (EI^+) ($[M\text{-}Br^-]^+$) calcd. for 410.3027, found: 410.3027.

3. NMR Spectra of relevant compounds

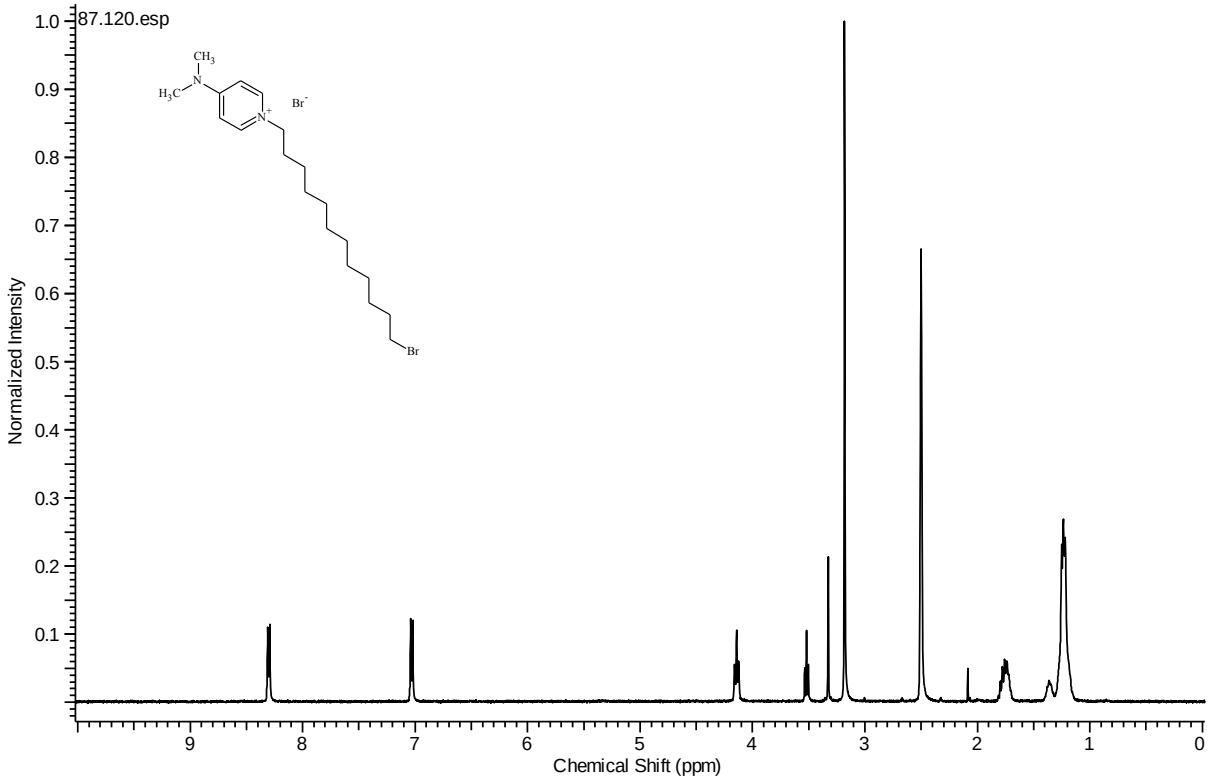

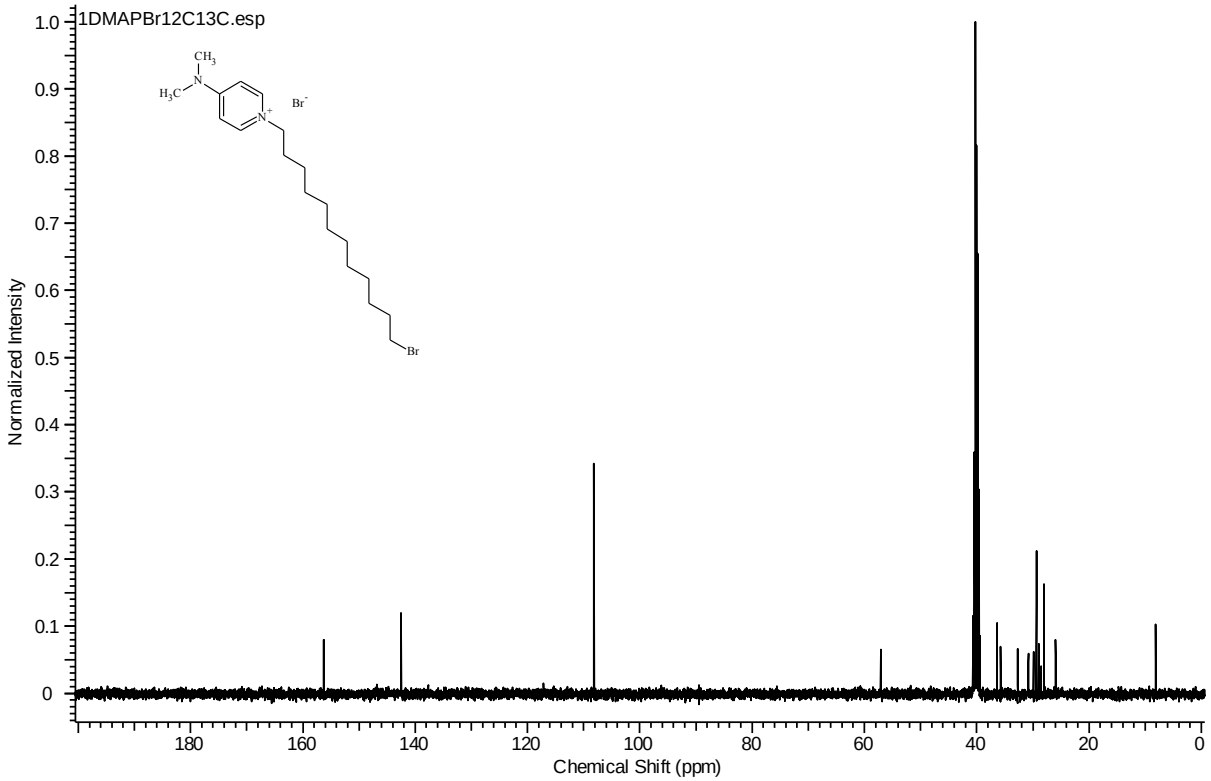

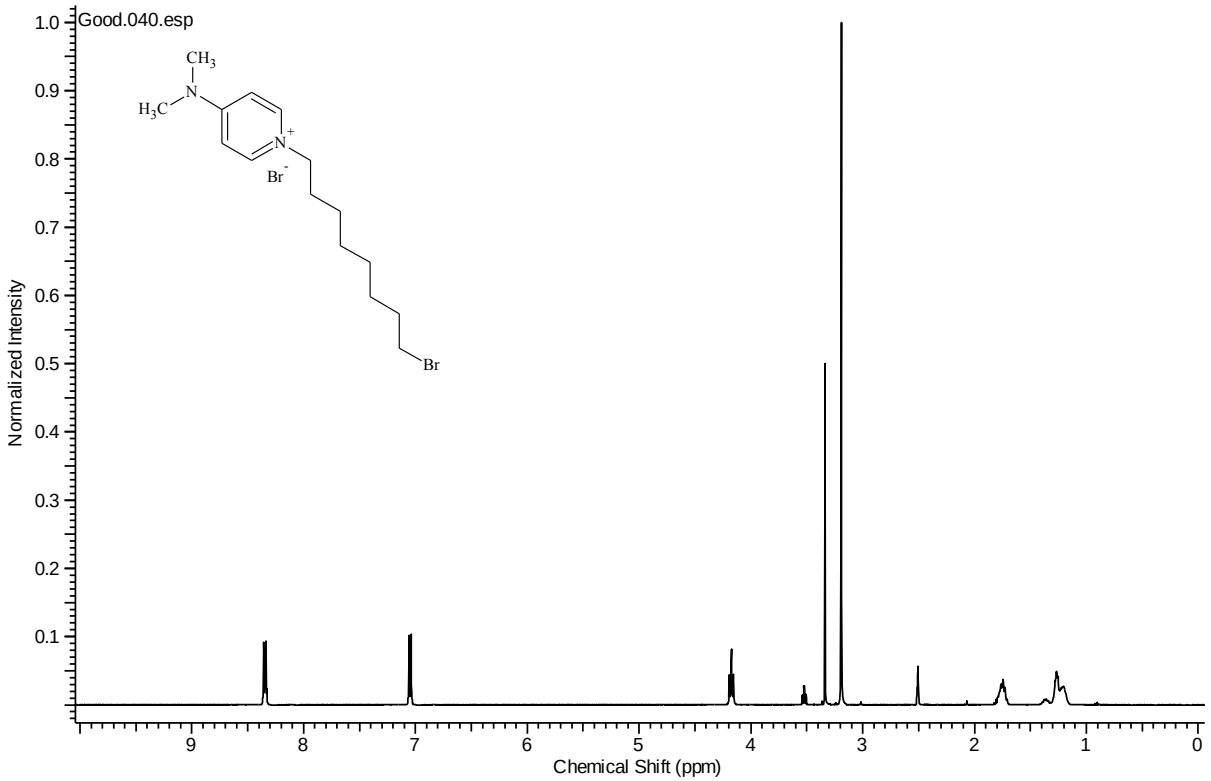
Good.040.esp
Normalized Intensity
Chemical Shift (ppm)
CH3
H3C
N
N+
Br-
Br

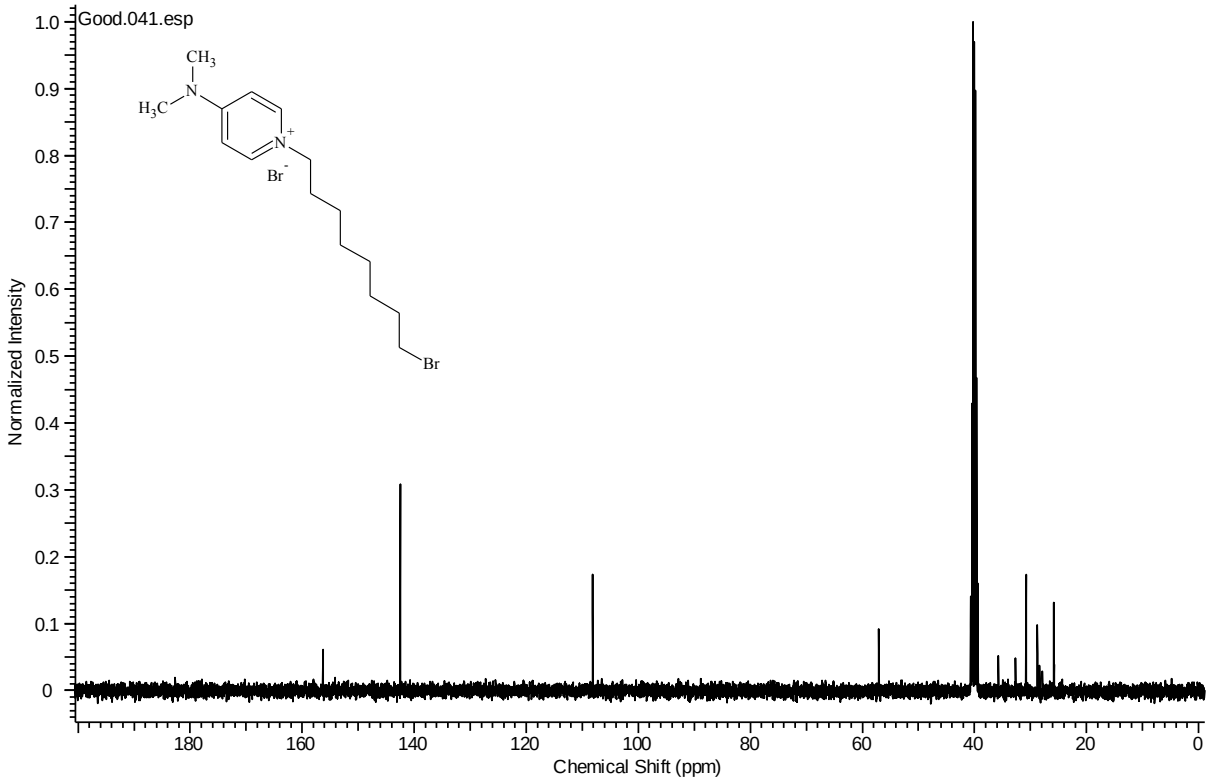
Good.041.esp
Normalized Intensity
Chemical Shift (ppm)
CH3
H3C
N
N+
Br-
Br

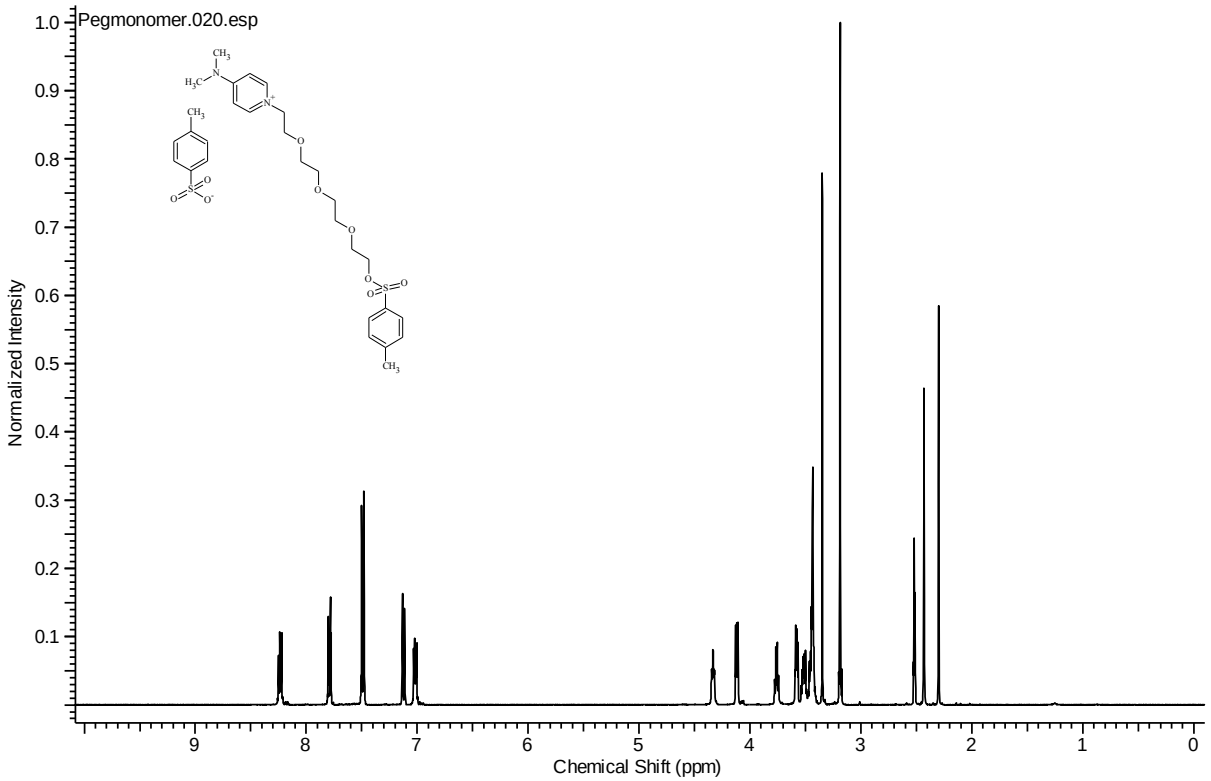
Pegmonomer.020.esp
Normalized Intensity
Chemical Shift (ppm)

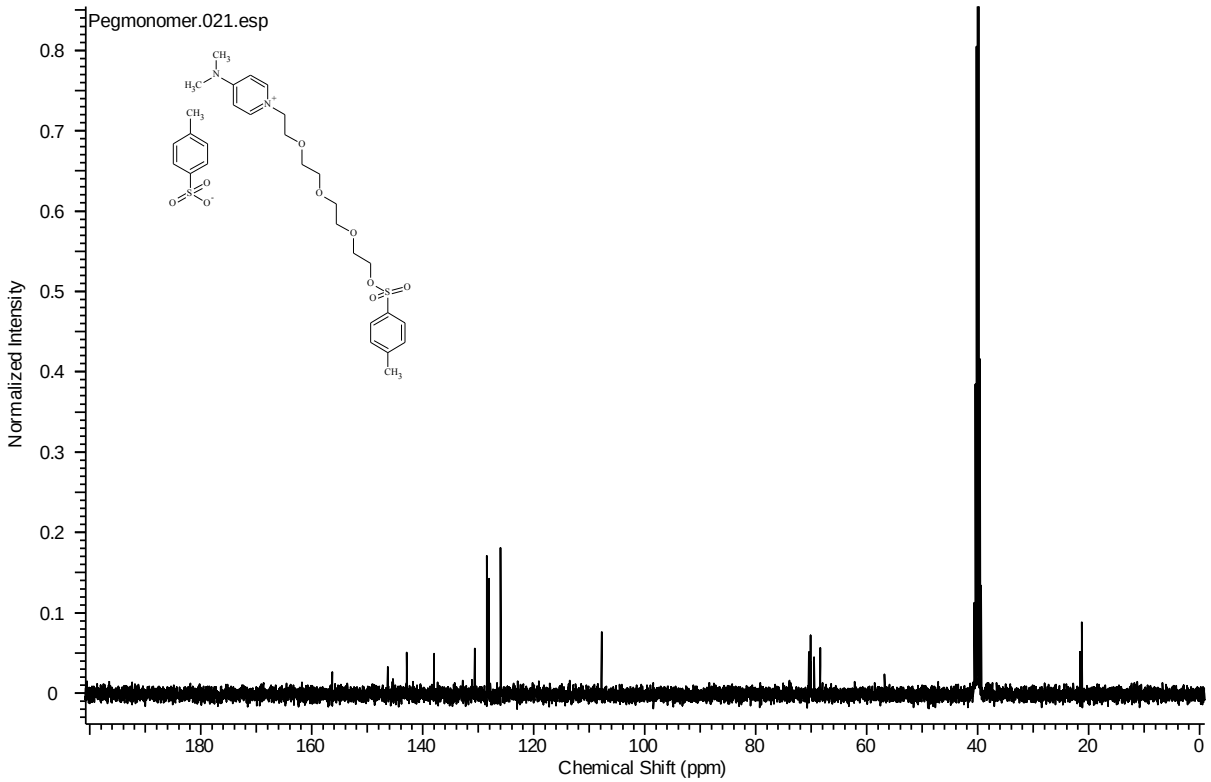
Pegmonomer.021.esp
Normalized Intensity
Chemical Shift (ppm)

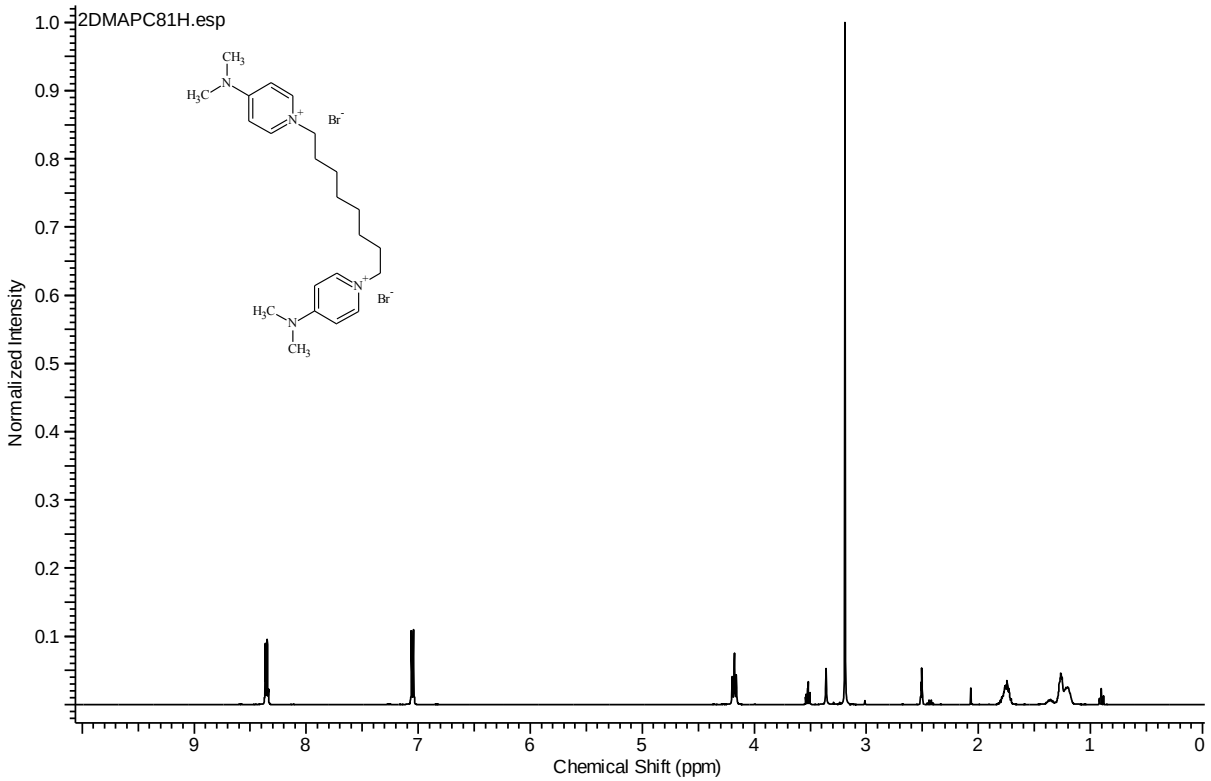
2DMAPC81H.esp
Normalized Intensity
Chemical Shift (ppm)

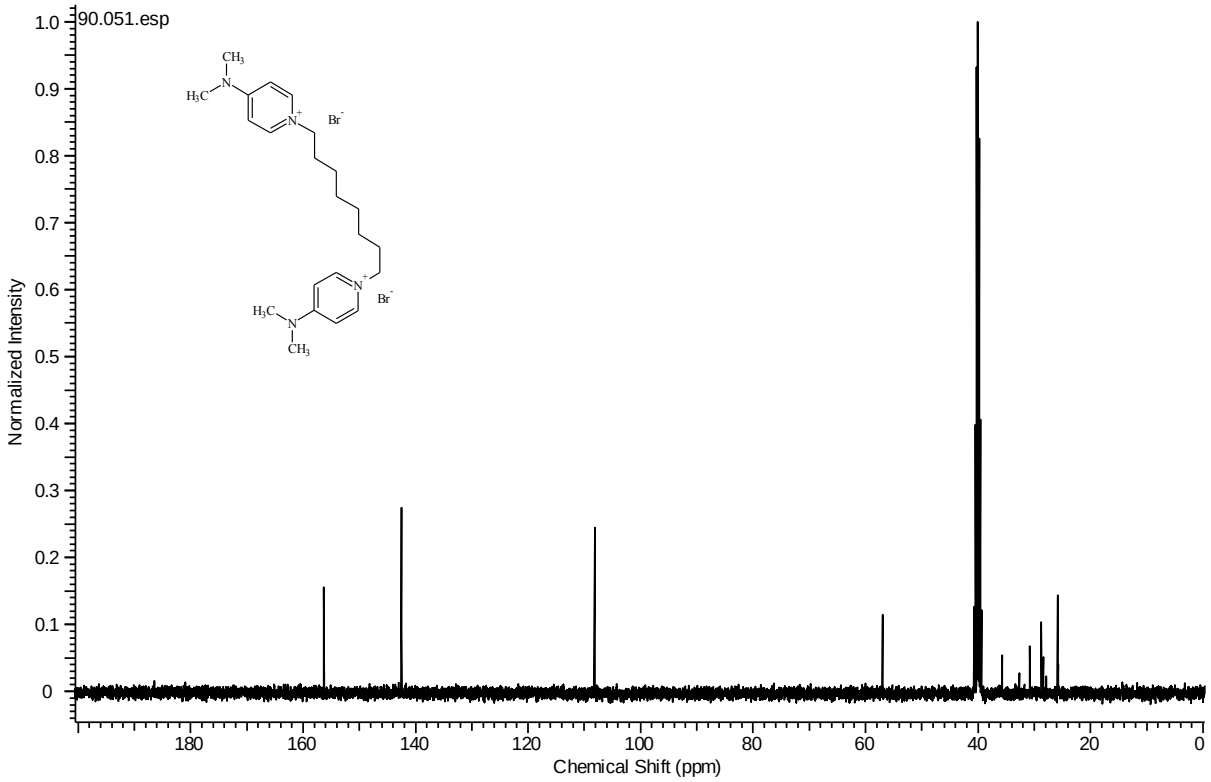
90.051.esp
Normalized Intensity
Chemical Shift (ppm)

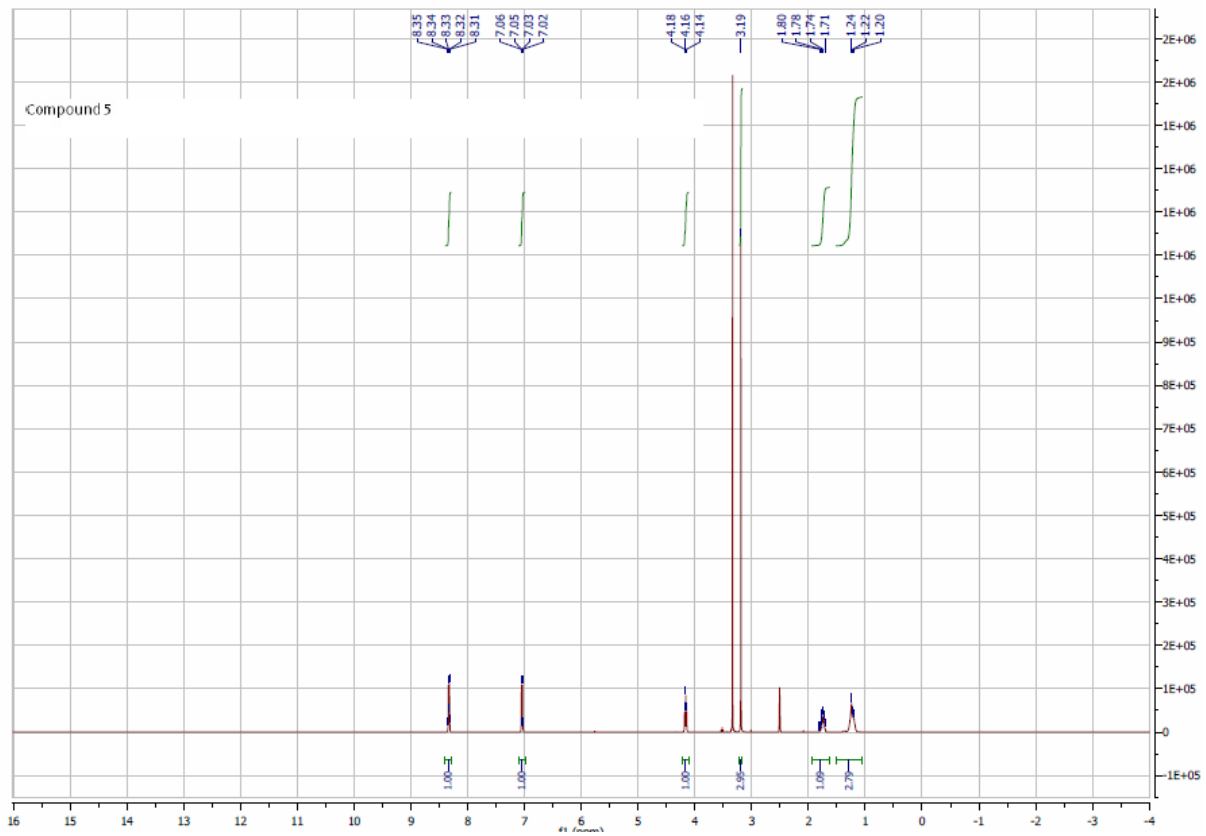
Compound 5
8.35
8.34
8.33
8.32
8.31
7.06
7.05
7.03
7.02
4.18
4.16
4.14
3.19
1.80
1.78
1.74
1.71
1.24
1.22
1.20
1.00
1.00
1.00
2.99
1.09
2.79

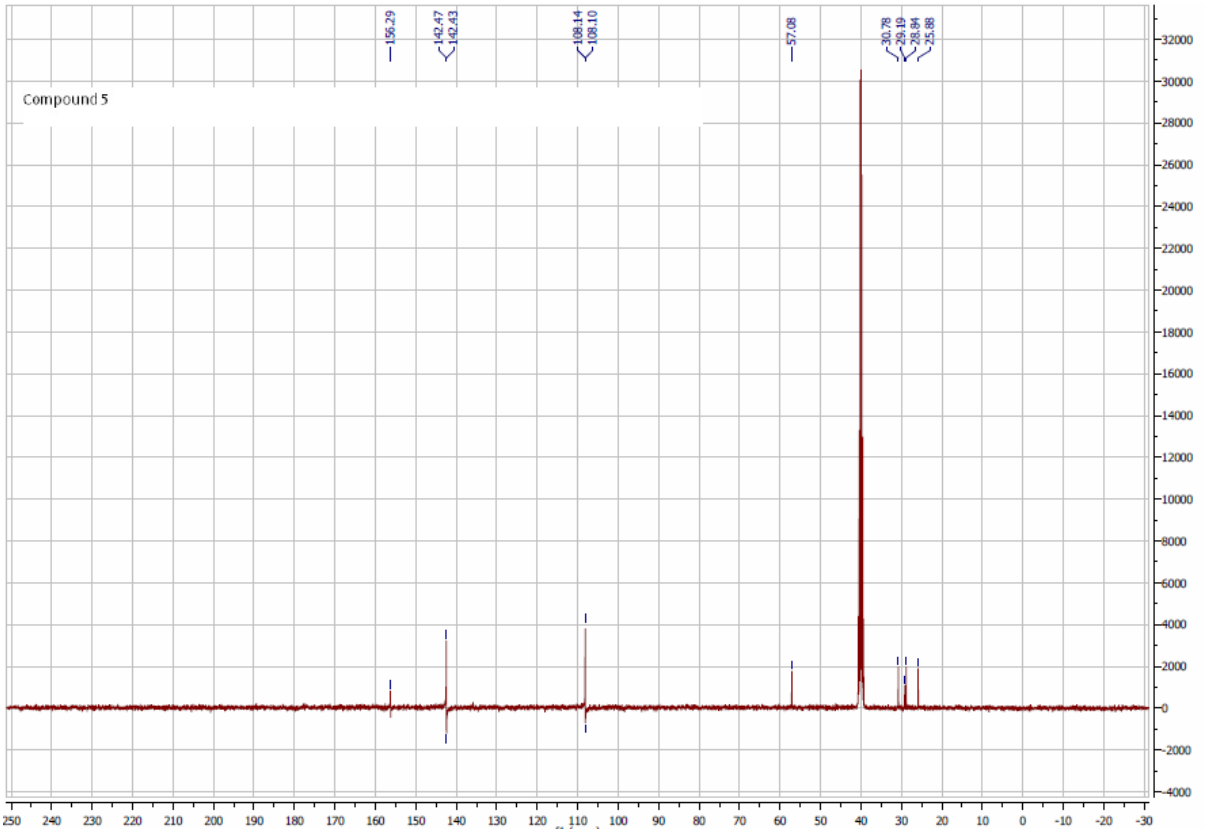
Compound 5
156.29
142.47
142.43
108.14
108.10
57.08
30.78
29.19
28.84
25.88

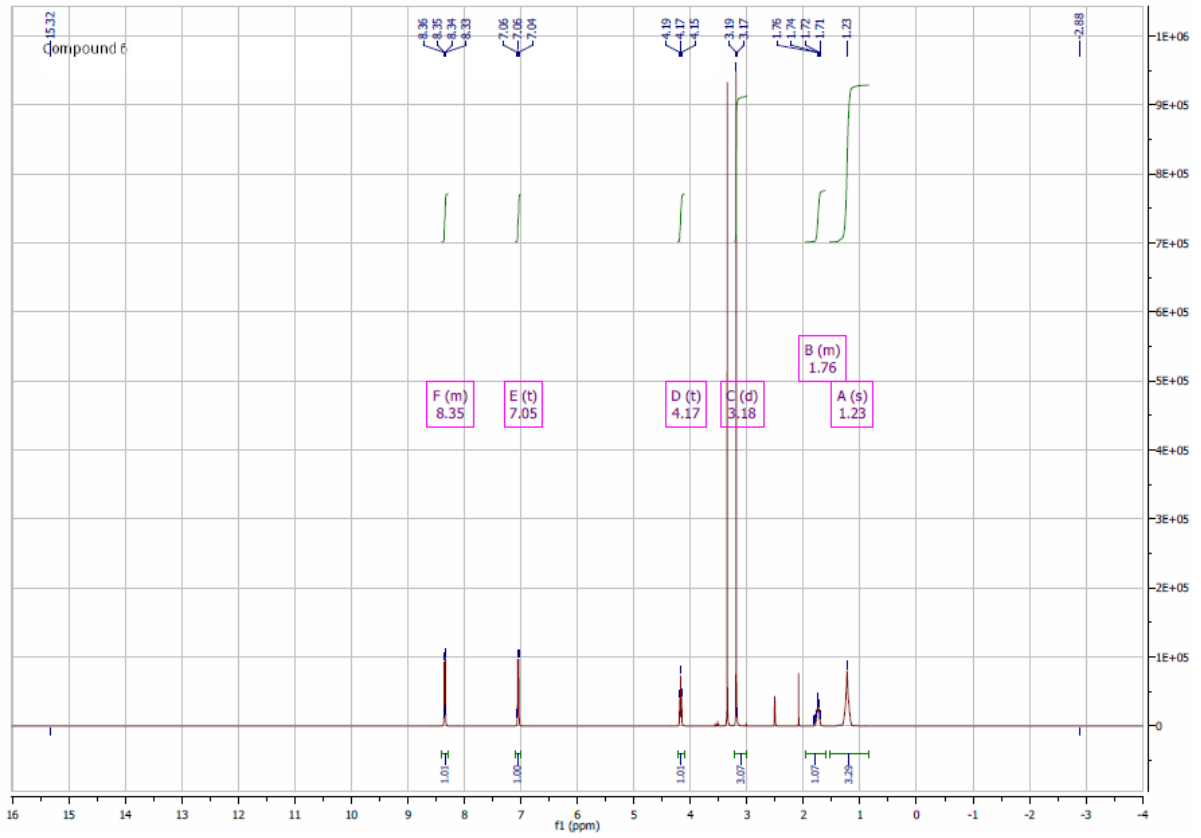
Compound 6
F (m)
8.35
E (t)
7.05
D (t)
4.17
C (d)
3.18
B (m)
1.76
A (s)
1.23
f1 (ppm)

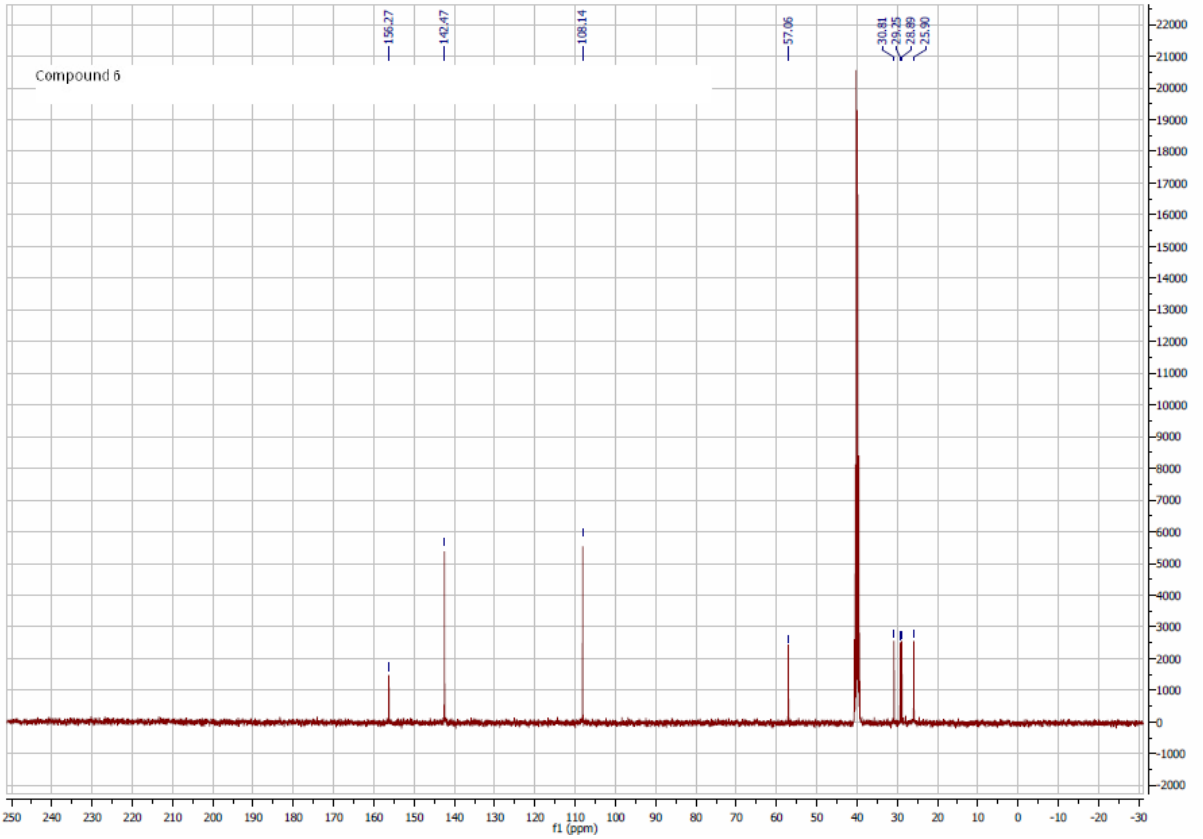
Compound 6
f1 (ppm)

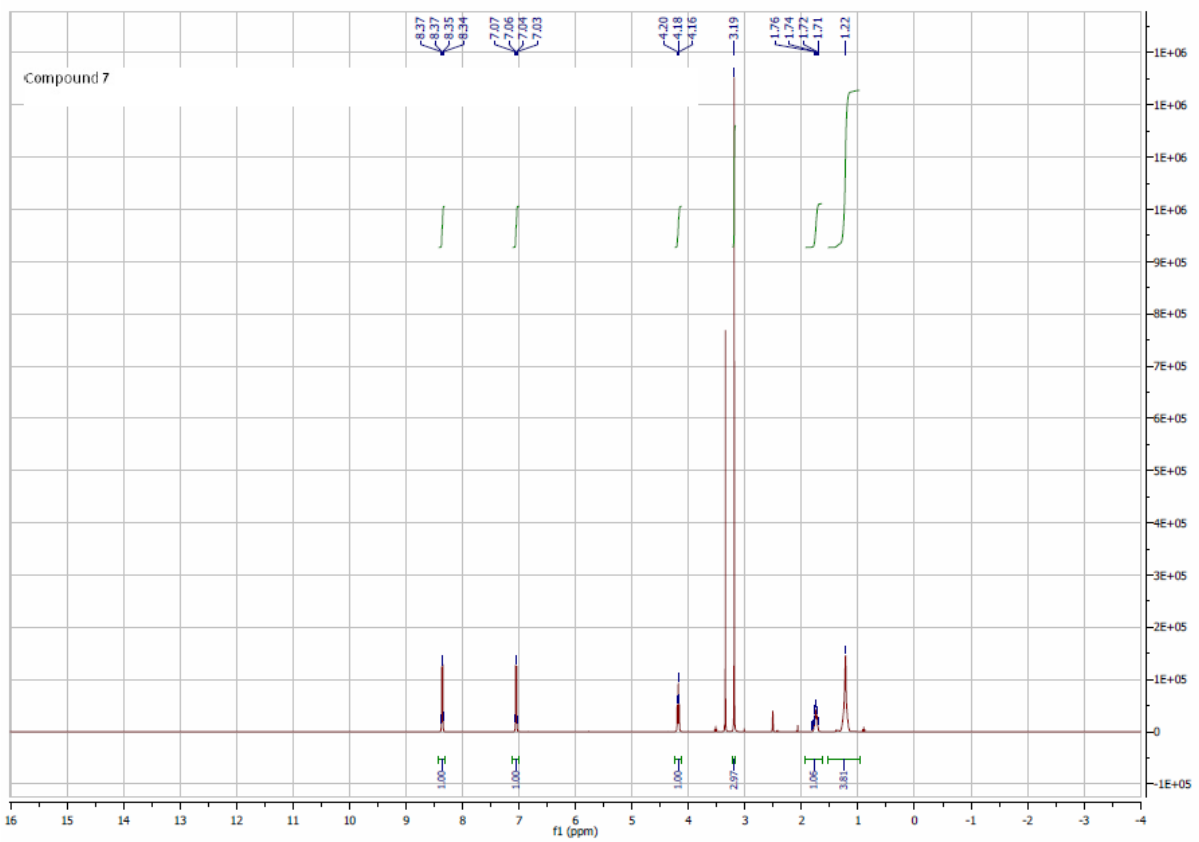
Compound 7
8.37
8.37
8.35
8.34
7.07
7.06
7.04
7.03
4.20
4.18
4.16
3.19
1.76
1.74
1.72
1.71
1.22
1.00
1.00
1.00
2.97
1.06
3.81
f1 (ppm)

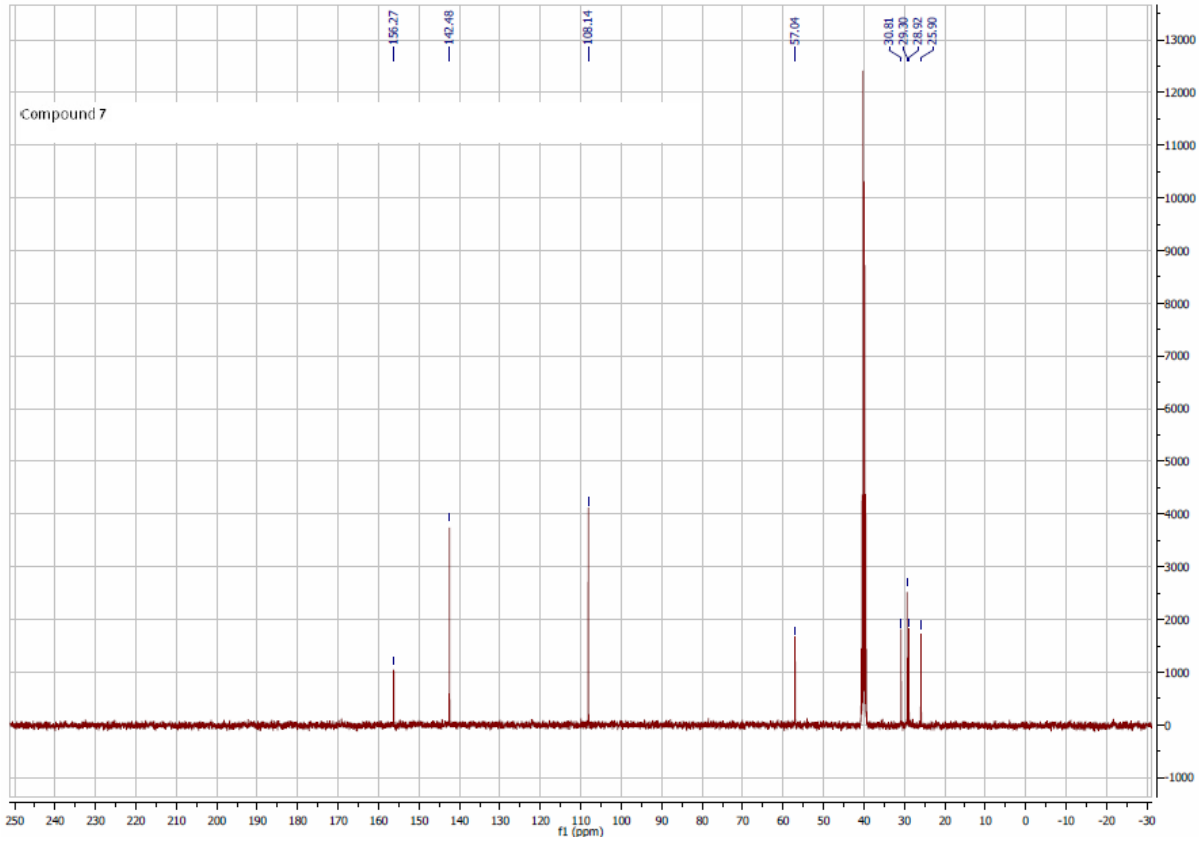
Compound 7
156.27
142.48
108.14
57.04
30.81
29.30
28.92
25.90
f1 (ppm)

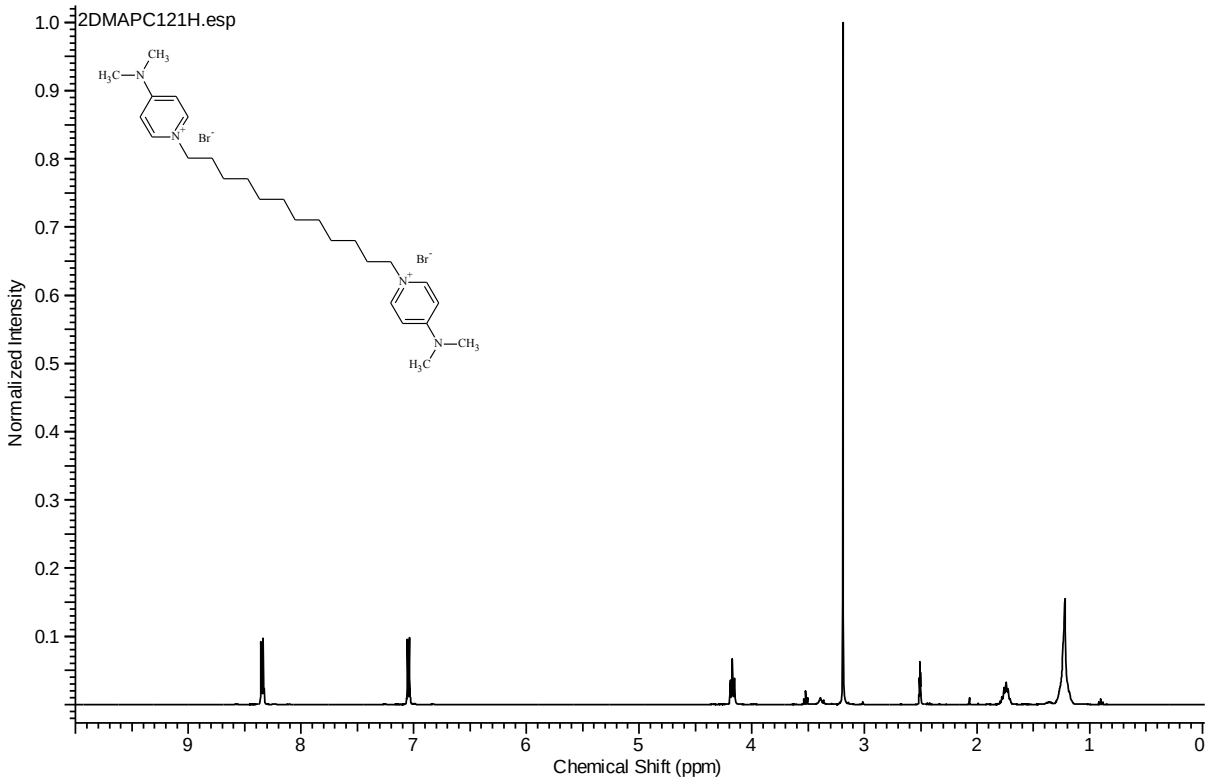
2DMAPC121H.esp
Normalized Intensity
Chemical Shift (ppm)

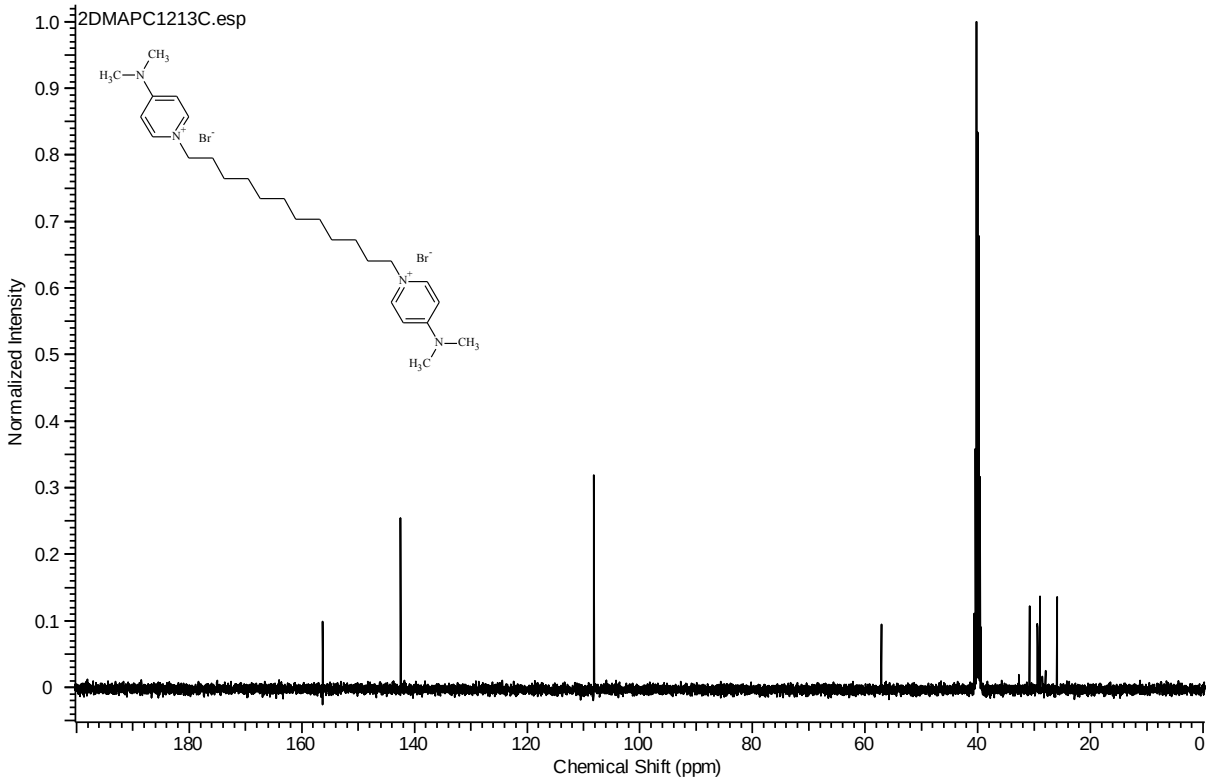
2DMAPC1213C.esp
Normalized Intensity
Chemical Shift (ppm)

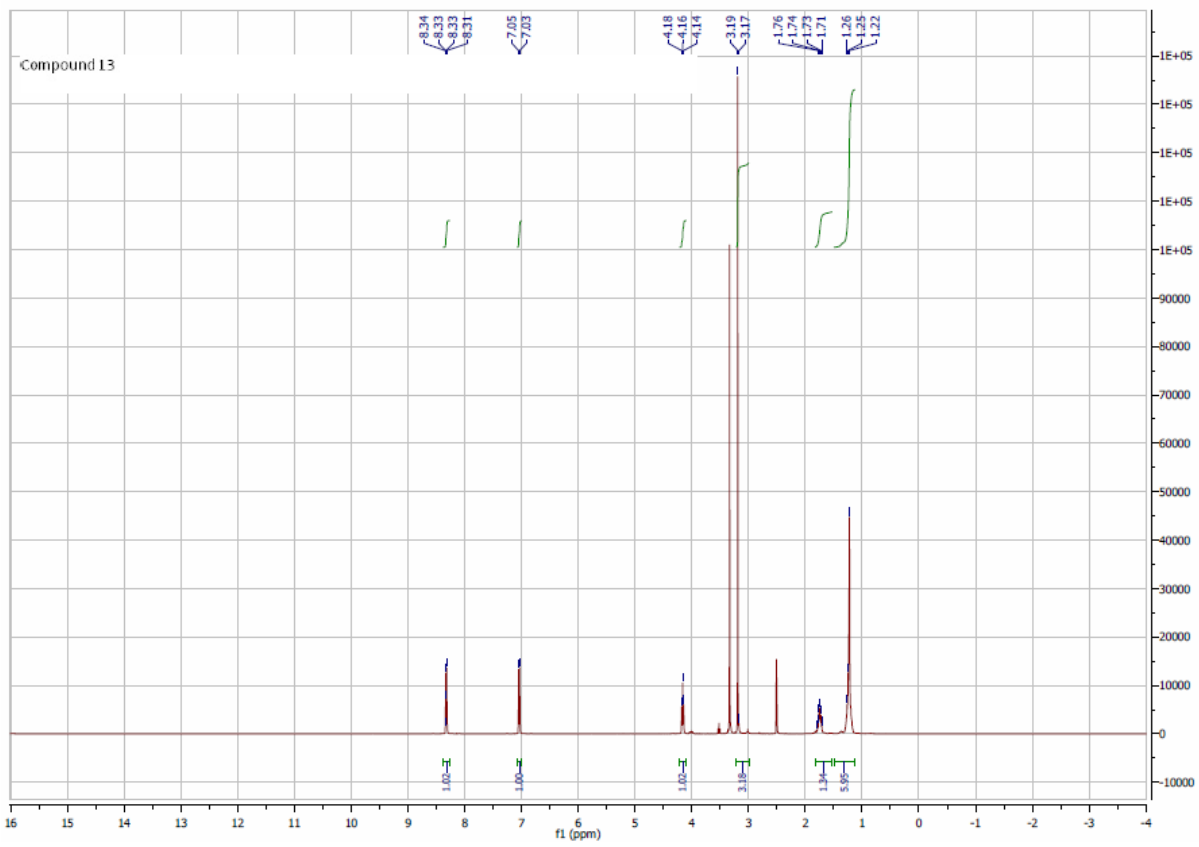
Compound 13
8.34
8.33
8.33
8.31
7.05
7.03
4.18
4.16
4.14
3.19
3.17
1.76
1.74
1.73
1.71
1.26
1.25
1.22
1.02
1.00
1.02
3.18
1.34
5.95
f1 (ppm)

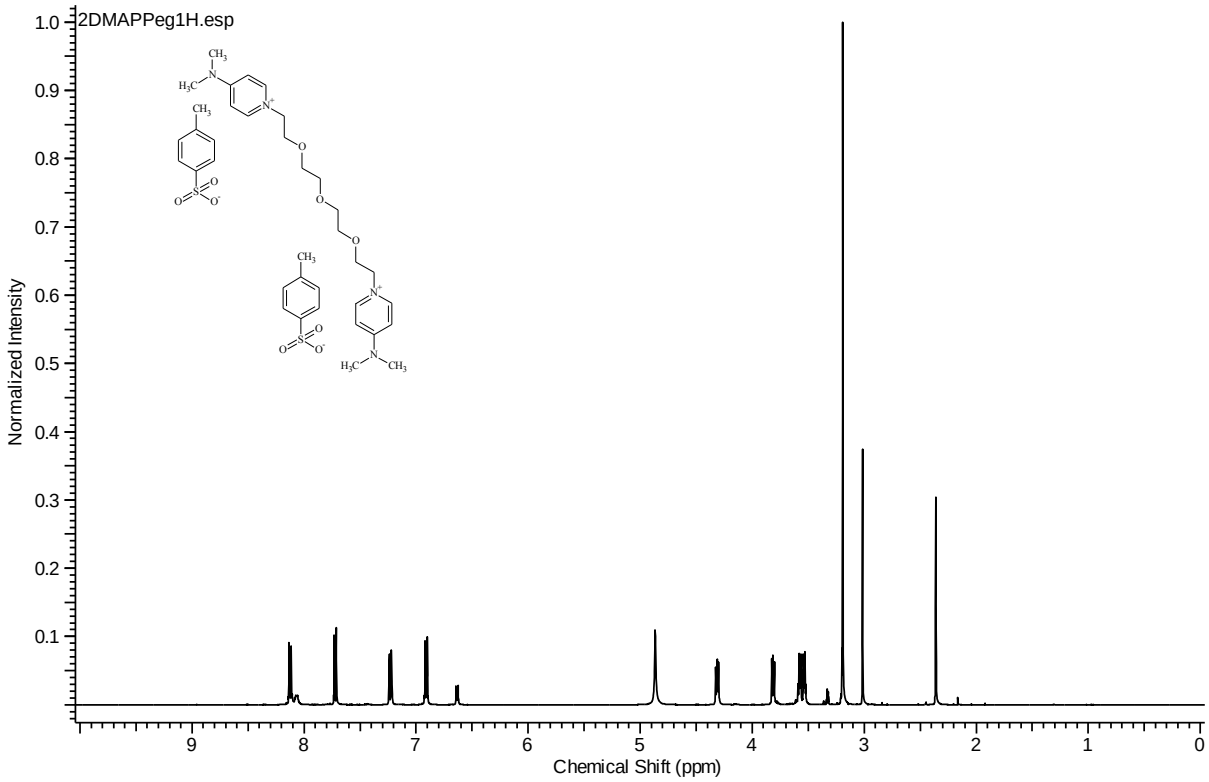
2DMAPPeg1H.esp
Normalized Intensity
Chemical Shift (ppm)

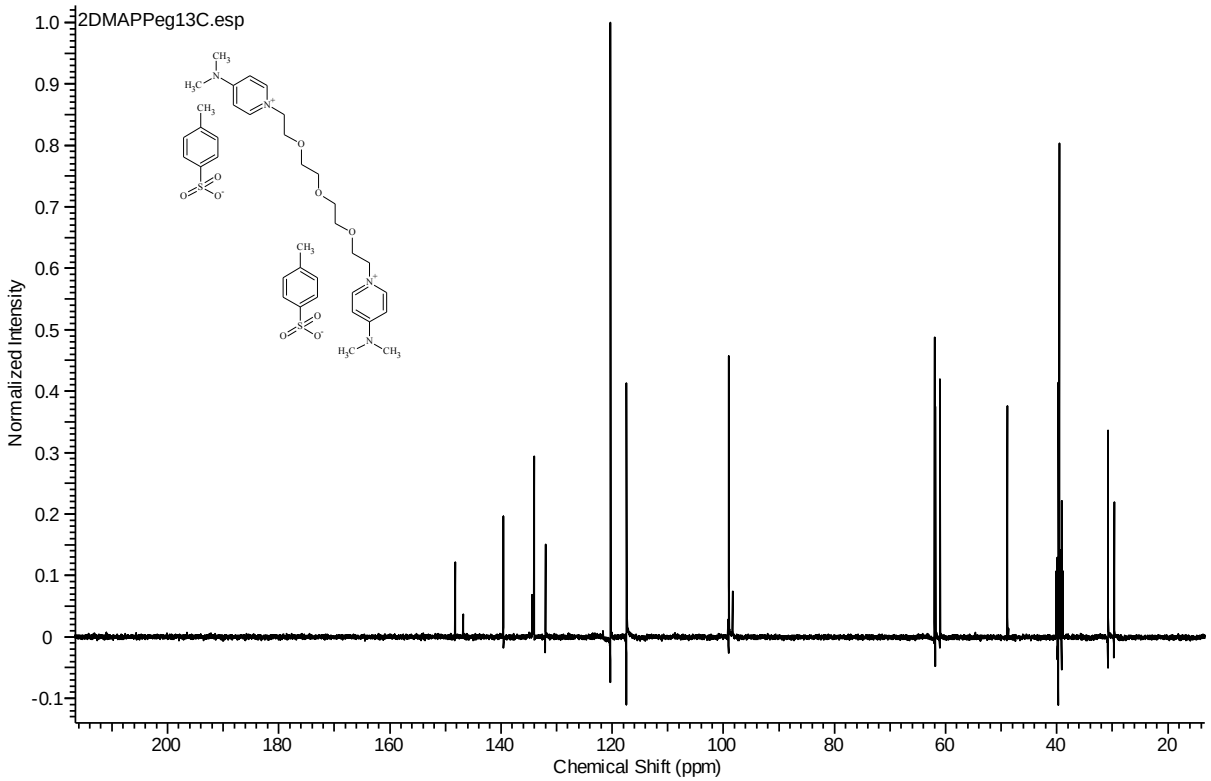
2DMAPPeg13C.esp
Normalized Intensity
Chemical Shift (ppm)

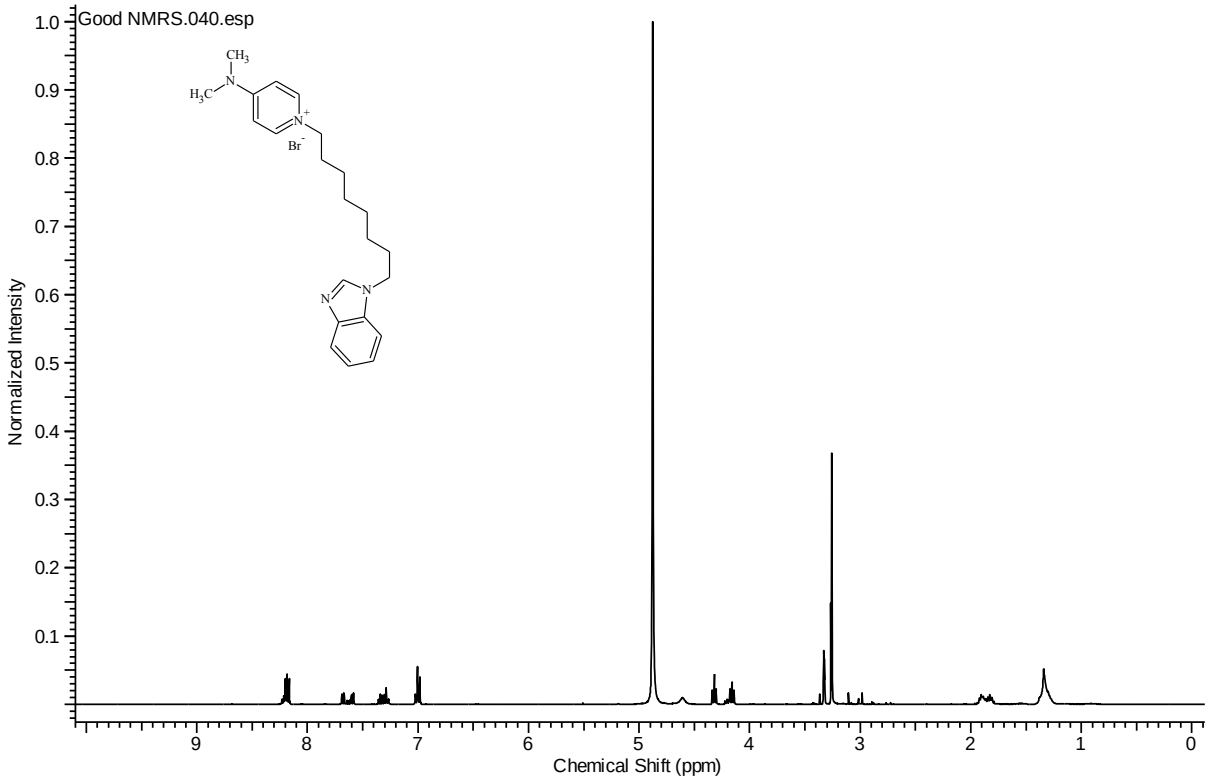
Good NMRS.040.esp
Normalized Intensity
Chemical Shift (ppm)

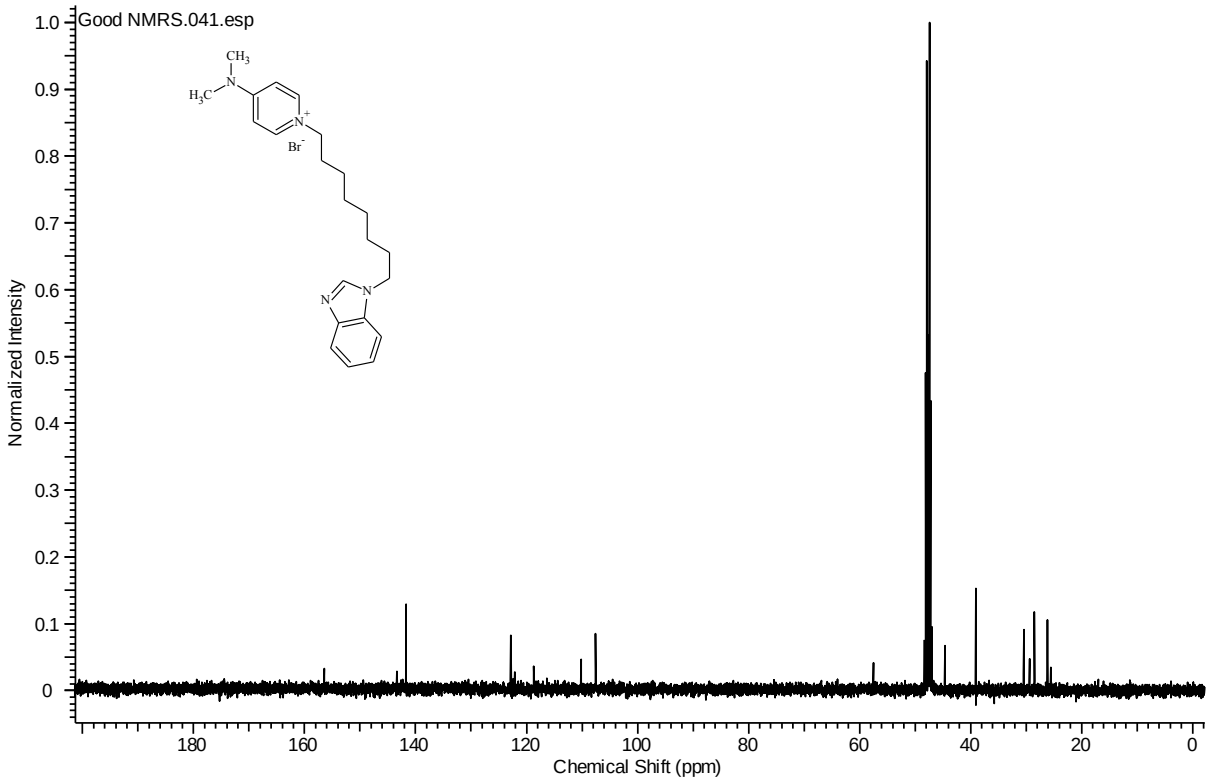
Good NMRS.041.esp
Normalized Intensity
Chemical Shift (ppm)
1.0
0.9
0.8
0.7
0.6
0.5
0.4
0.3
0.2
0.1
0
180
160
140
120
100
80
60
40
20
0

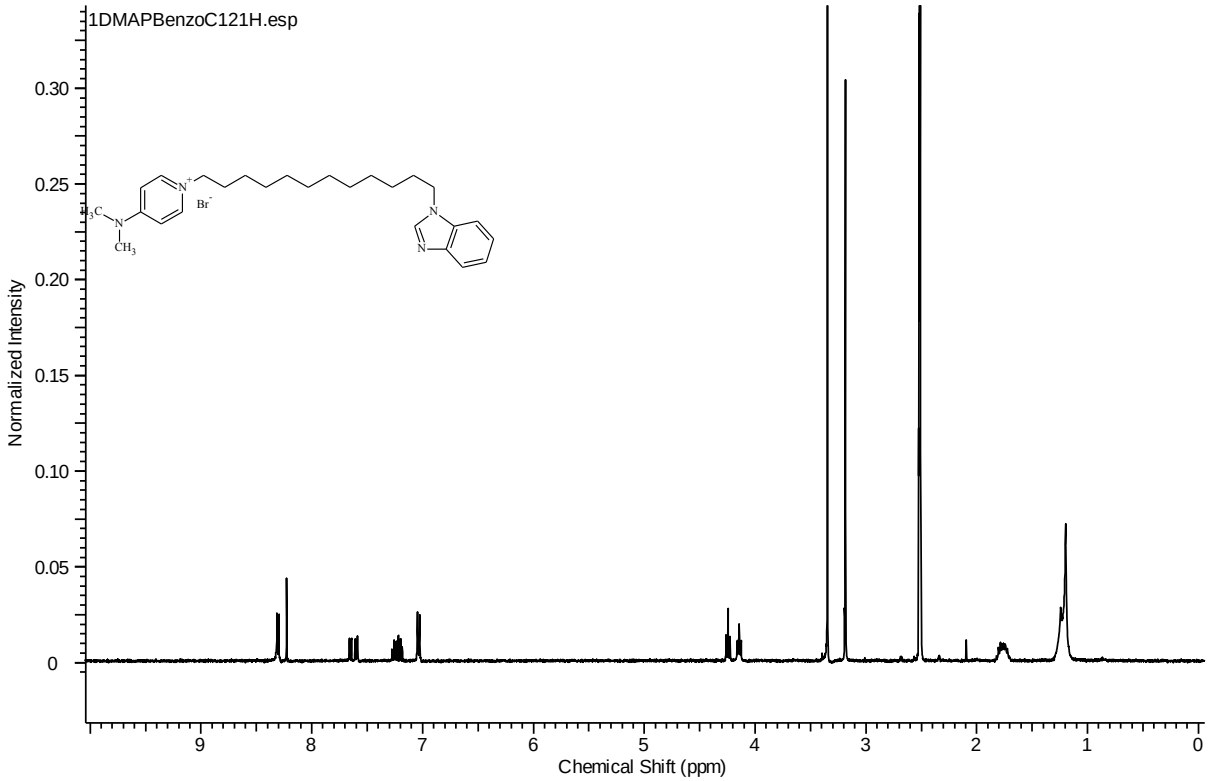
1DMAPBenzoC121H.esp
Normalized Intensity
Chemical Shift (ppm)

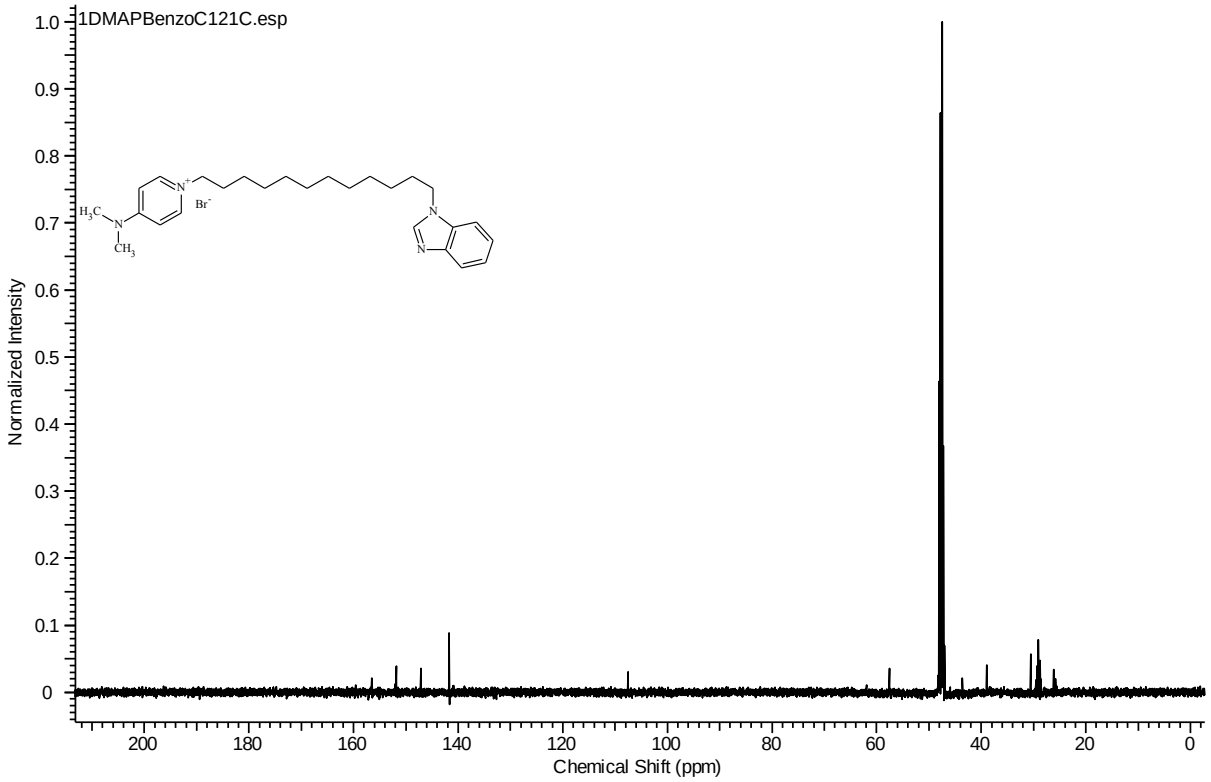
1DMAPBenzoC121C.esp
Normalized Intensity
Chemical Shift (ppm)

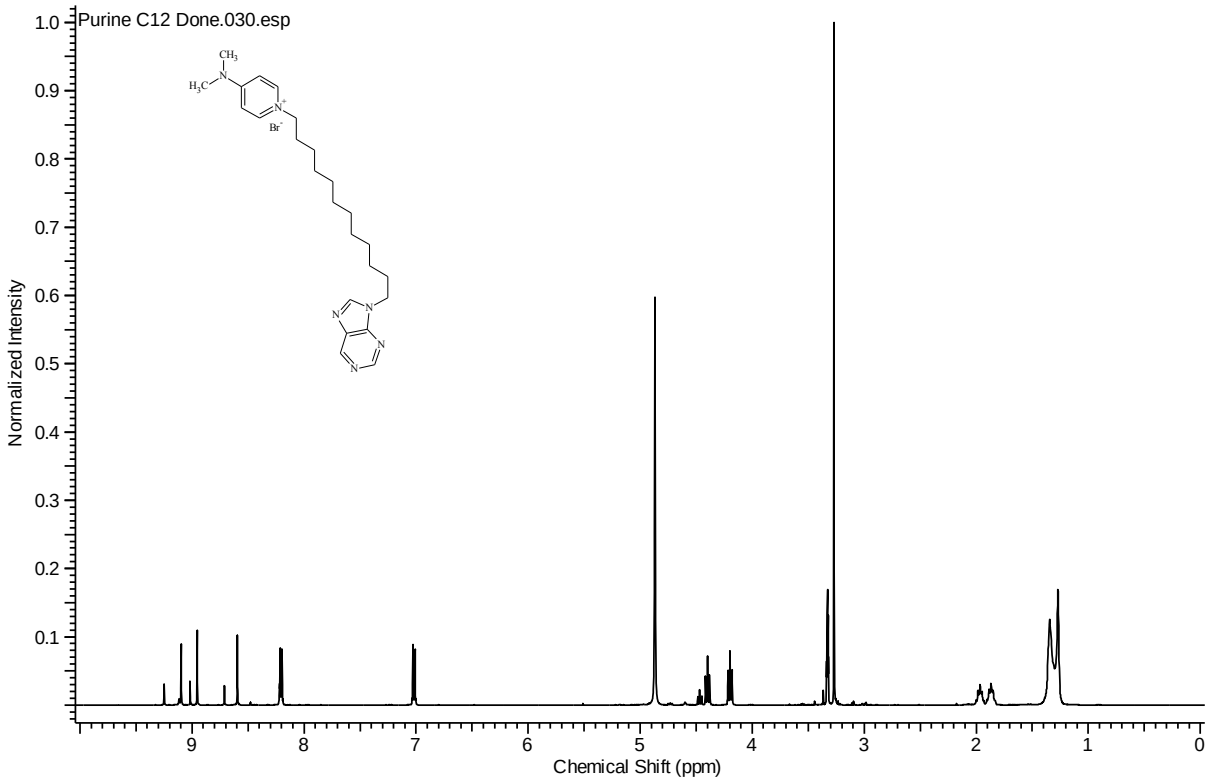
Purine C12 Done.030.esp
Normalized Intensity
Chemical Shift (ppm)

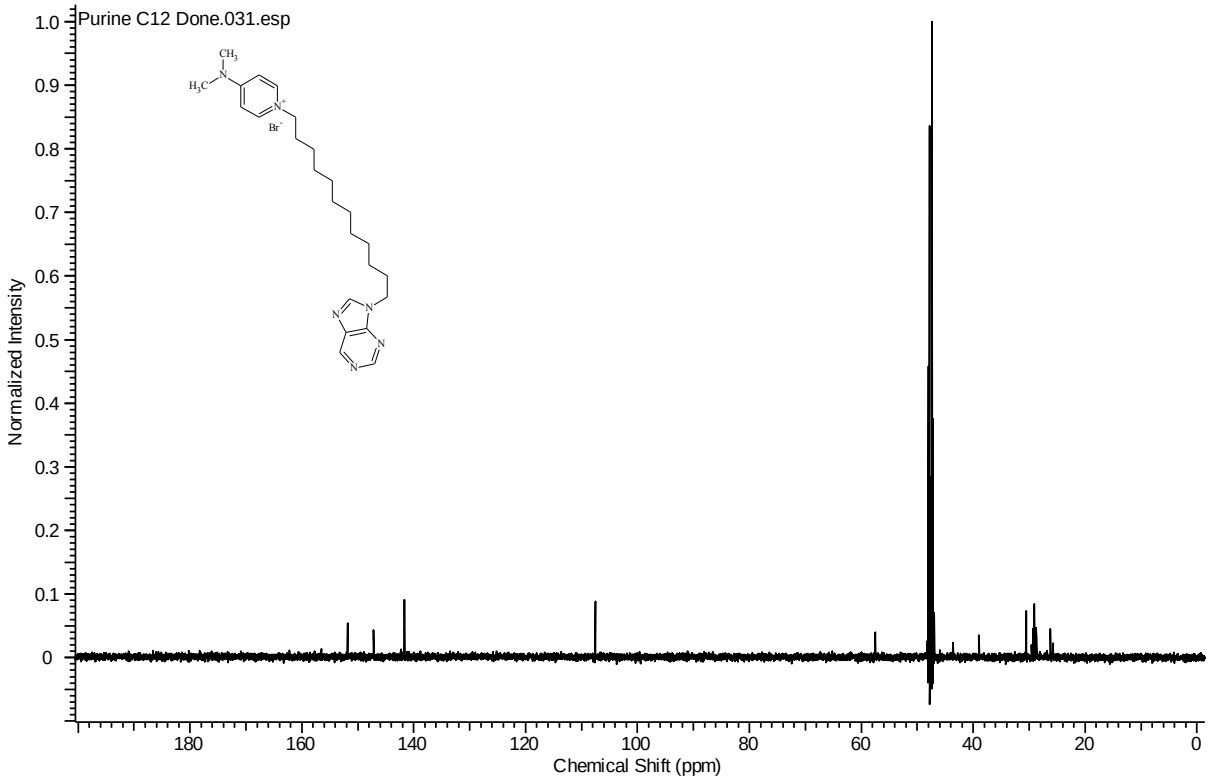
Purine C12 Done.031.esp
Normalized Intensity
Chemical Shift (ppm)

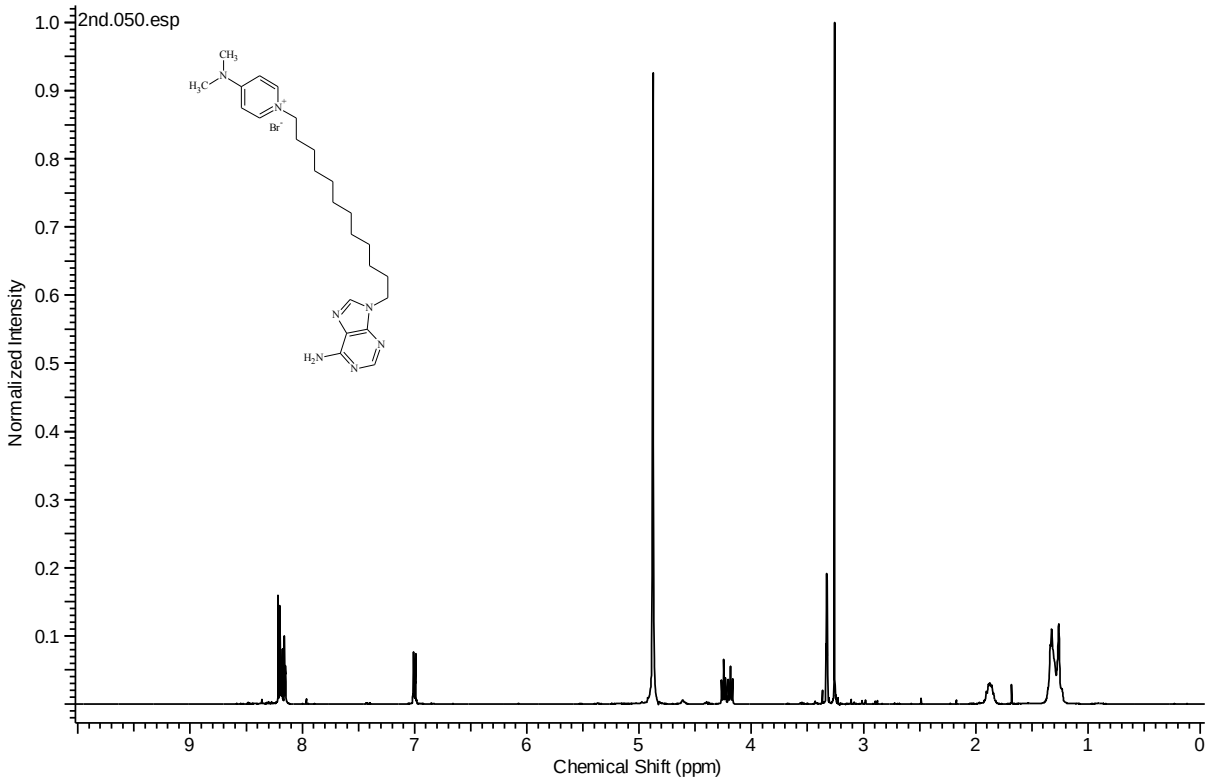
2nd.050.esp
Normalized Intensity
Chemical Shift (ppm)

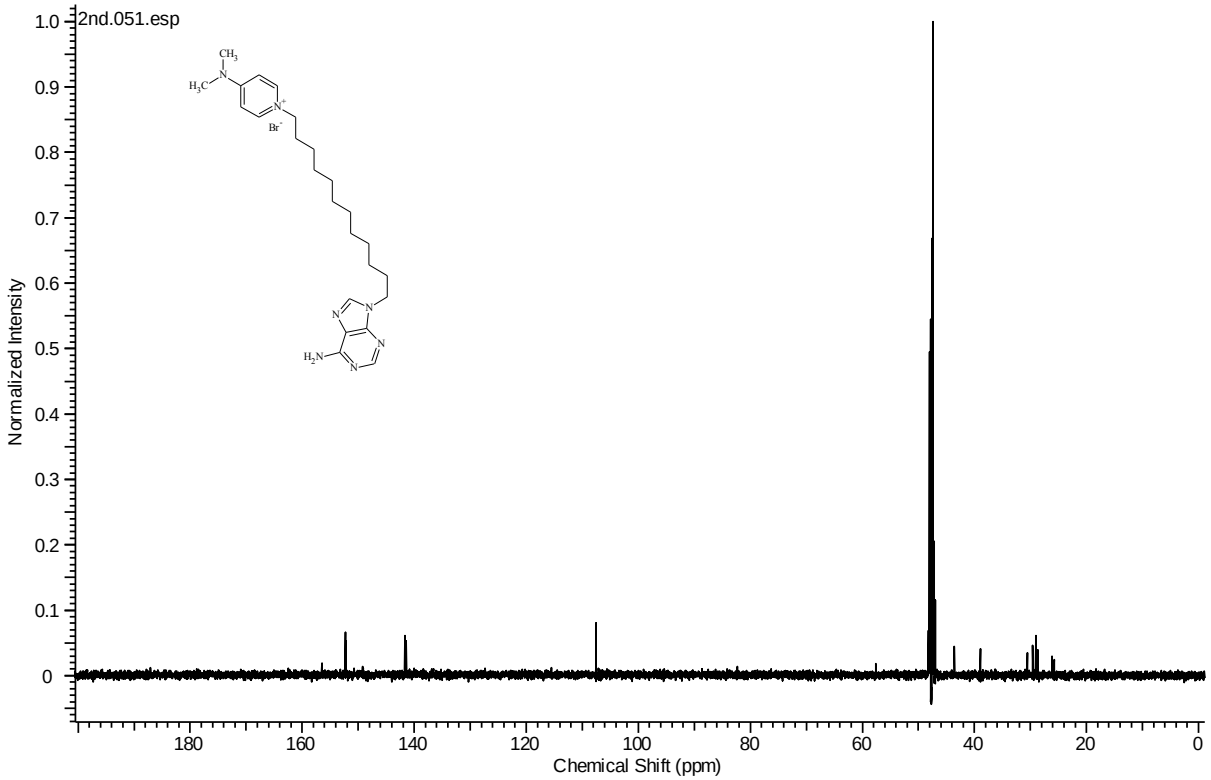
2nd.051.esp
Normalized Intensity
Chemical Shift (ppm)

4. Molecular modelling

All calculations were performed at Imperial College High Performance Computing cluster. Ligands were drawn in ChemDraw and imported into Maestro (version 9.2.112, Schrodinger Inc.) and prepared using the LigPrep and Epik (pH 7±2) and the OPLS2005 force field. The protein was imported from the PDB-database (3G15.pdb). Chain A was used throughout the study and the Protein Preparation Wizard was used to remove water molecules, to add hydrogens, hydrogen bonding network optimisation and finally for a restrained energy minimisation. For some dockings two water molecules close to the biding site of hemicholinium that connects Asp306, Asn345 and Glu349 and Arg444 were kept, as well as one water molecule that is involved in bridging hydrogen bonding between the carboxylate of Glu206 and N7 of ADP. Docking grids were constructed from the resulting proteins using the grid generator in GLIDE. The box was placed around hemicholinium and ADP (virtually connected via a carbon chain bond into a single ligand for convenient positioning of the box around the site). The size of the grid box was adjusted to dock ligands <36Å. Docking of the inhibitors **3-13** (compound **7** in multiple protonation states) was performed with GLIDE in standard precision (SP) or extra precision (XP) mode, sample nitrogen inversions, sample ring conformations (2.5 kcal/mol) and expanded sampling. 15000 poses per ligand were kept during the initial state and 800 were kept for energy minimisation (dielectric constant 2.0 and maximum minimisation steps 1000). The van der Waals radii of the ligands were scaled with 0.8 and with a partial cut-off of 0.15. No constraints were used. The ligand interaction diagram script (Schrodinger Inc.) was used to generate 2D-representations of the binding modes. For subsequent scoring of the docked ligands with the molecular mechanics generalized Born surface area (MM-GBSA) method the Prime module within Schrodinger was used. The flexible residues including the water molecule within 5Å from the ligand were minimised with a harmonic constraint applied. All non-flexible residues were frozen. The Ligand interaction diagram tool was used to construct the Supplementary Figures 3, 4 and 5.

Docking was evaluated both in the presence and in the absence of ADP and crystal water molecules in close proximity to the binding site. The presence or absence of the water molecules that connects Asp306, Asn345 and Glu349 and Arg444 did not alter the binding poses significantly, however removal of the water molecule in the ATP-site resulted in the loss of a hydrogen bond and lower scores, hence in subsequent dockings the water molecule in the ATP site was kept. The docking algorithm could successfully dock the co-crystallised hemicholinium (RMSD = 0.3 Å) both in the presence and in the absence of ADP (Supplementary Figure 3). For compound **3**, **5**, **6**, **8** and **13** that docked simultaneously to the choline site and the rim of the pocket Glide XP docking and MM-GBSA scoring of the best poses gave excellent correlation between the estimated free energy of binding and experimental IC_{50} values. (Supplementary Figure 2 and Supplementary Table 1). XP docking of compound **7** resulted in an unrealistic pose, however, with SP docking and subsequent XP refinement and MM-GBSA scoring also this compound fitted the model well. Compound **9**, **10** and **12** docked simultaneously to the choline site and the ATP site in their highest scored poses and as expected these compounds did not fit the previous binding model (Supplementary Table 1).

5. Biological Methods

Enzyme assay

Choline kinase activity was measured using a modified spectrophotometric pyruvate kinase/lactate dehydrogenase-coupled assay.[1] Δ49N CHKA2 was a kind gift of Arnon Lavie (University of Illinois) and Manfred Konrad (Max Planck Institute for Biophysical Chemistry). In a total volume of 50 µL, 20 ng enzyme was subjected to reaction buffer containing 72 µM choline (K_M), 450 µM ATP (K_M), 100 mM Tris pH 7.5, 100 mM KCl, 10 mM $MgCl_2$, 500 µM phosphoenolpyruvate, 4 units pyruvate kinase, 5 units lactate dehydrogenase and 250 µM NADH (all from Sigma-Aldrich) in the presence of varying concentrations of inhibitor. The reaction was carried out at 37°C in UV-star 96-well microplates (Greiner Bio-one) and initiated by addition of reaction buffer. ADP formation was indirectly measured by detection of NADH depletion at 340 nm on a Tecan Infinite M200 microplate reader. Half maximal inhibitory concentrations (IC_{50}) were calculated by fitting of sigmoidal curves with variable slope by least squares (ordinary) fitting method in GraphPad Prim version 5.01.

The mode of inhibition was determined by Lineweaver-Burk plots. To assess competitiveness with choline, ATP was kept constant at 450 µM, while choline concentrations were varied between 40 µM and 20 mM. Competitiveness with ATP was determined by keeping choline constant at 72 µM while varying ATP concentrations between 10 µM and 5 mM. Both experiments were carried out in absence or presence of 0.1, 1, 10 µM inhibitor. Double reciprocal plots of substrate concentrations versus velocity were obtained as described elsewhere[2] and linear regression (best fit by minimised sum of squares) performed in GraphPad Prism version 5.01. Due to the endogenous ATPase activity of CHKA2, which results in higher than anticipated velocity at low substrate concentrations, data are curved in some cases where the lowest substrate concentration had to be excluded once reciprocal velocity changed in non-linear fashion.

Cell culture and growth inhibition assay

HCT-116 colon cancer cells (ATCC) were cultured in RPMI-1640 (Invitrogen) supplemented with 10% foetal calf serum (Lonza), glutamine, penicillin and streptomycin (all Invitrogen). A549 lung cancer cells (ATCC) were maintained in DMEM (Invitrogen) supplemented with 10% foetal calf serum, glutamine, penicillin and streptomycin. St-T1b cells were maintained in DMEM/F12 (Invitrogen) supplemented with 10% foetal calf serum, glutamine, penicillin and streptomycin. Cell lines were incubated at 37°C in a humidified atmosphere containing 5% CO_2. Half-maximal growth inhibitory concentrations (GI_{50}) were determined using sulforhodamine B (SRB) assay as described elsewhere.[3] In brief, cells were seeded in 96-wells plates and after 24 hours treated in six replicates with medium or 9 different concentrations of inhibitor and incubated for additional 72 hours. Cells were fixed with 10% trichloroacetic acid and stained with 0.4% sulforhodamine B in 1% acetic acid. The stained protein was solubilised in 10 mM Tris (all from Sigma-Aldrich) and optical densities measured at 540 nm using a Multiskan EX spectrophotometer (Thermo Scientific). Growth inhibition curves were plotted as percentage of control cells and GI_{50} determined by fitting a sigmoidal curve with variable slope by least squares (ordinary) fitting method in GraphPad Prism version 5.01.

Whole-cell choline kinase activity assay

Inhibitor-dependent reduction of choline kinase activity in whole cells was determined in HCT-116 cells by monitoring the decrease of phosphocholine formation following a modified Bligh and Dyer extraction described elsewhere.[4] In brief, HCT-116 cells were seeded in 6-well plates and treated with 0.16, 0.8, 4, 20 and 100 µM inhibitor for 1 hour and pulsed with 1 µCi [^{3}H]-choline chloride (PerkinElmer) at 0.5 µCi/mL for an additional hour. Cells were washed 3 times in cold PBS and 750 µL of methanol/chloroform (2:1; both from Sigma-Aldrich) added. The solubilised cytosolic content was transferred into microcentrifuge tubes and 200 µL H_2O added. Samples were centrifuged for 10 minutes and 750 µL supernatant transferred to fresh microcentrifuge

tubes. 250 µL chloroform and 250 µL H_2O were added and samples vortexed and centrifuged. 650 µL of the upper aqueous phase were transferred to a fresh microcentrifuge tube and 500 µL 12 mM sodium phosphate (pH 7.0) and 750 µL 5 mg/mL tetraphenylborate (TPB) in heptan-4-one (all from Sigma-Aldrich) added. Samples were vortexed and the phases separated through centrifugation. The choline-containing upper phase was discarded and any residual choline was re-extracted with 500 µL TPB from the lower phosphocholine phase. After vortexing and centrifugation, 200 µL of the lower aqueous phase were added to 3.8 mL of Ultima Gold™ scintillation cocktail (PerkinElmer) and radioactivity measured on a scintillation counter. [^{3}H]Phosphocholine content was normalised to protein as determined by BCA assay (Pierce) and compared to drug-naïve control cells.

Western blotting

Cells were lysed in RIPA buffer containing protease and phosphatase inhibitors (all from Sigma-Aldrich). 20 µg protein was resolved on a 4-15% mini-protean TGX gel (Biorad) and transferred to a PVDF membrane (Trans-Blot Turbo Transfer Packs, Biorad). Membranes were blocked for 1 hour in 5% milk in tris-buffered saline containing 0.1% v/v tween (TBST, Cell Signaling) and incubated with anti-CHKA (Sigma-Aldrich, HPA024153) or β-actin (Abcam, ab6276) antibody overnight at 4°C. Secondary HRP conjugated mouse and rabbit antibodies (Santa Cruz Biotechnology) were applied for one hour at room temperature. Signals were visualised using Amersham ECL™ Western Blotting Detection Reagent (GE Healthcare Life Sciences) and Amersham Hyper-film (GE Healthcare Life Sciences).

References

1. E. Malito, N. Sekulic, W. C. Too, M. Konrad and A. Lavie, *J Mol Biol*, 2006, **364**, 136-151.

2. V. Gomez-Perez, T. McSorley, W. C. See Too, M. Konrad and J. M. Campos, *ChemMedChem*, 2012, **7**, 663-669.

3. V. Vichai and K. Kirtikara, *Nat Protoc*, 2006, **1**, 1112-1116.

4. J. J. Murray, T. T. Dinh, A. P. Truett, 3rd and D. A. Kennerly, *Biochem J*, 1990, **270**, 63-68.